Random Discrete Morse Theory and a New Library of Triangulations

Bruno Benedetti and Frank H. Lutz

Abstract

(1) We introduce random discrete Morse theory as a computational scheme to measure the complicatedness of a triangulation. The idea is to try to quantify the frequence of discrete Morse matchings with a certain number of critical cells. Our measure will depend on the topology of the space, but also on how nicely the space is triangulated.

(2) The scheme we propose looks for optimal discrete Morse functions with an elementary random heuristic. Despite its naïveté, this approach turns out to be very successful even in the case of huge inputs.

(3) In our view the existing libraries of examples in computational topology are 'too easy' for testing algorithms based on discrete Morse theory. We propose a new library containing more complicated (and thus more meaningful) test examples.

1 Introduction

Libraries of objects for algorithm testing are extremely common in computational geometry. Their set-up requires particular care: If a library consists of objects 'too easy to understand', then basically any algorithm would score great on them, thus making it impossible for the researcher to appreciate the efficiency of her algorithms. Of course, agreeing on what examples should be regarded as 'easy' is a hard challenge, and how to quantify complicatedness is even harder.

In the present paper, we focus on computational topology, which deals with simplicial complexes in an abstract manner, i.e., without prescribing a shape, a volume, or the dimension of a Euclidean space in which they embed. We present a possible statistical approach, which we call *random discrete Morse theory*. The mathematical background relies on Forman's discrete Morse theory from 1998 [27, 28], which in turn builds on Whitehead's simple homotopy theory, developed around 1939 [73]. (Especially important is Whitehead's notion of collapsibility, which is a combinatorial strengthening of the contractibility property.)

Our idea is to create a quantitative version of these two theories. For example, we would like to be able to tell not only if a complex is collapsible or not, but also 'how easy it is' to find a collapsing sequence. To give a mathematical basis to this intuition, we consider a random model where we perform elementary collapses completely at random. The likelihood to find a complete collapsing sequence this way, will measure how easy it is to collapse the complex. Although this likelihood is, in most cases, too difficult to compute, we can estimate it empirically in polynomial time. The following elementary heuristic takes also into account complexes that are not contractible.

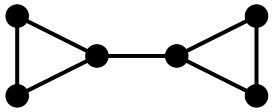

Figure 1: The graph A_7.

ALGORITHM: RANDOM DISCRETE MORSE

INPUT: A d-dimensional (abstract, finite) simplicial complex C, given by its list of facets.

(0) Initialize $c_0 = c_1 = \ldots = c_d = 0$.
(1) Is the complex empty? If yes, then STOP; otherwise, go to (2).
(2) Are there free codimension-one faces? If yes, go to (3); if no, go to (4).
(3) *Elementary Collapse*: Pick one free codimension-one face uniformly at random and delete it, together with the unique face that contains it. Go back to (1).
(4) *Critical Face*: Pick one of the top-dimensional faces uniformly at random and delete it from the complex. If i is the dimension of the face just deleted, increment c_i by 1 unit. Go back to (1).

OUTPUT: The resulting discrete Morse vector $(c_0, c_1, c_2, \ldots, c_d)$.

By construction, c_i counts the critical faces of dimension i. According to Forman [27], any discrete Morse vector $(c_0, c_1, c_2, \ldots, c_d)$ is also the face vector of a cell complex homotopy equivalent to C.

Definition 1 *The* discrete Morse spectrum *of a (finite) simplicial complex C is the collection of all possible resulting discrete Morse vectors produced by the algorithm* RANDOM DISCRETE MORSE *together with the distribution of the respective probabilities.*

Example: Consider the graph A_7 of Figure 1 above. As there are no free vertices in it, RANDOM DISCRETE MORSE picks an edge uniformly at random and deletes it. If the edge chosen is the central bridge (which happens with probability $\frac{1}{7}$), the output discrete Morse vector is $(2, 3)$. If any other edge than the central one is chosen, the output vector is $(1, 2)$. The discrete Morse spectrum is therefore $\{\frac{6}{7}\text{-}(1, 2),\ \frac{1}{7}\text{-}(2, 3)\}$; or, shortly, $\{(1, 2), (2, 3)\}$ if we simply want to list the vectors of the spectrum.

The algorithm RANDOM DISCRETE MORSE requires no backtracking, and 'digests' the complex very rapidly. The output $(1, 0, 0, \ldots, 0)$ is a certificate of collapsibility. If the output is different from $(1, 0, \ldots, 0)$, the complex could still be collapsible with a different sequence of free-face deletions. Every optimal discrete Morse vector has some positive probability to appear as output of the algorithm; unfortunately, this probability can be arbitrarily small. In case optimality is not reached, the algorithm still outputs something meaningful, namely (as already mentioned) the f-vector of a cell complex homotopy equivalent to the given complex.

Since the output arrives quickly, we can re-launch the program, say, 10000 times, possibly on separate computers (independently). The distribution of the obtained outcomes yields an approximation of the discrete Morse spectrum. By the so-called Morse inequalities, each output vector is componentwise larger or equal than the vector of Betti numbers $(\beta_0, \ldots, \beta_d)$. When the spectrum stays 'close' to the vector of Betti numbers, we can regard the triangulation to be easy. This allows an empirical analysis of how complicated the complex is.

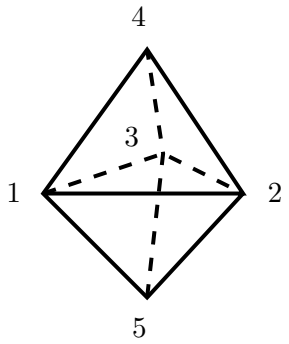

Figure 2: The bipyramid.

We point out that the problem of finding *optimal* discrete Morse functions (with as fewest critical cells as possible) is NP-hard [35, 44]; even the decision problem of whether some given (connected, finite) simplicial complex is collapsible or not is NP-complete [69]. We therefore *should not* expect to immediately find optimal discrete Morse vectors for any input. Indeed, one can easily construct examples on which our (or similar) random heuristic performs poorly; see Appendix A.

However, for many triangulations of *huge* size, our elementary random heuristic produces optimal discrete Morse functions in almost 100% of the runs of the program. This could be interesting in the future also for homology computations. Discrete Morse functions (for general cell complexes) are implicitly computed in several homology algorithms that are based on fast (co-)reduction techniques, like the packages CHomP [20], RedHom [17], and Perseus [64].

The paper is structured as follows: First we give details of our algorithm (Section 2) and compare it with previous approaches (Section 3). Then we survey the existing topological and combinatorial lower bounds for optimal discrete Morse vectors (Section 4). Finally, we describe and examine a collection of examples coming from several different areas of topology (Section 5). In our opinion, the resulting library (Appendix B) is a richer and more sensitive testing ground for implementations based on discrete Morse theory.

2 Details of the algorithm and computational complexity

In the following, we give a more explicit description of our random heuristic.

The first thing we do is to build the Hasse diagram of the given simplicial complex C, which represents the incidence structure of the face poset of C; see Figure 3 for an example. It takes $O(d \cdot I \cdot T)$ steps to construct the Hasse diagram of a simplicial complex, in case the complex is given by its facets (or to be precise, by its vertex-facet incidences). Here d is the dimension of the input complex, T the total number of faces, and I the number of vertex-facet-incidences [37]; cf. also [38].

Once the upward Hasse diagram and the downward Hasse diagram are set up (see below), we deconstruct a copy of the upward Hasse diagram in every run of our program by deleting (randomly picked) critical faces or pairs of faces in case there are free faces. We illustrate this with a concrete example.

Example 2 (The bipyramid) The 2-dimensional boundary of the bipyramid of Figure 2 has 6 triangles, 9 edges, and 5 vertices. We list the faces level-wise in lexicographic order

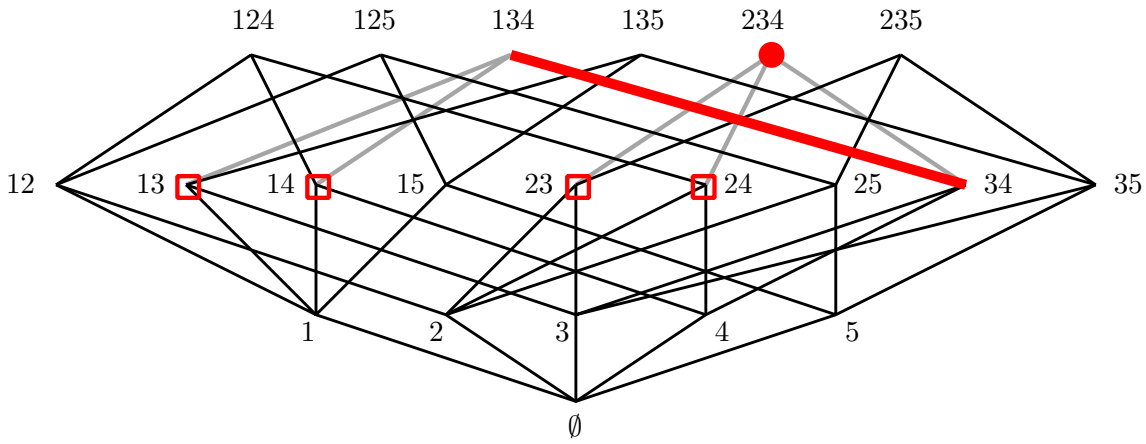

Figure 3: The Hasse diagram of the bipyramid with one critical triangle (234), one matching edge (34–134), and four free edges (13, 14, 23, 24) highlighted.

and identify each face by a label k^i denoting the k-th face of dimension i in the respective lexicographic list.

$$1^2\text{: [1,2,4]},\ 2^2\text{: [1,2,5]},\ 3^2\text{: [1,3,4]},\ 4^2\text{: [1,3,5]},\ 5^2\text{: [2,3,4]},\ 6^2\text{: [2,3,5]},$$
$$1^1\text{: [1,2]},\ 2^1\text{: [1,3]},\ 3^1\text{: [1,4]},\ 4^1\text{: [1,5]},\ 5^1\text{: [2,3]},\ 6^1\text{: [2,4]},\ 7^1\text{: [2,5]},\ 8^1\text{: [3,4]},\ 9^1\text{: [3,5]},$$
$$1^0\text{: [1]},\ 2^0\text{: [2]},\ 3^0\text{: [3]},\ 4^0\text{: [4]},\ 5^0\text{: [5]}.$$

Next, we initialize the Hasse diagram. Hereby, the graph of the Hasse diagram is stored twice. In the *upward Hasse diagram*, we level-wise list all inclusions of i-dimensional faces in $(i+1)$-dimensional faces,

$i=1$: $1^1 \nearrow \{1^2, 2^2\},\ 2^1 \nearrow \{3^2, 4^2\},\ 3^1 \nearrow \{1^2, 3^2\},\ 4^1 \nearrow \{2^2, 4^2\},\ 5^1 \nearrow \{5^2, 6^2\},$
$6^1 \nearrow \{1^2, 5^2\},\ 7^1 \nearrow \{2^2, 6^2\},\ 8^1 \nearrow \{3^2, 5^2\},\ 9^1 \nearrow \{4^2, 6^2\},$

$i=0$: $1^0 \nearrow \{1^1, 2^1, 3^1, 4^1\},\ 2^0 \nearrow \{1^1, 5^1, 6^1, 7^1\},\ 3^0 \nearrow \{2^1, 5^1, 8^1, 9^1\},$
$4^0 \nearrow \{3^1, 6^1, 8^1\},\ 5^0 \nearrow \{4^1, 7^1, 9^1\},$

while in the *downward Hasse diagram* we level-wise list the $(j-1)$-dimensional faces that are contained in the j-dimensional faces,

$j=2$: $1^2 \searrow \{1^1, 3^1, 6^1\},\ 2^2 \searrow \{1^1, 4^1, 7^1\},\ 3^2 \searrow \{2^1, 3^1, 8^1\},$
$4^2 \searrow \{2^1, 4^1, 9^1\},\ 5^2 \searrow \{5^1, 6^1, 8^1\},\ 6^2 \searrow \{5^1, 7^1, 9^1\},$

$j=1$: $1^1 \searrow \{1^0, 2^0\},\ 2^1 \searrow \{1^0, 3^0\},\ 3^1 \searrow \{1^0, 4^0\},\ 4^1 \searrow \{1^0, 5^0\},\ 5^1 \searrow \{2^0, 3^0\},$
$6^1 \searrow \{2^0, 4^0\},\ 7^1 \searrow \{2^0, 5^0\},\ 8^1 \searrow \{3^0, 4^0\},\ 9^1 \searrow \{3^0, 5^0\}.$

Here, $3^1 \nearrow \{1^2, 3^2\}$ is the short notation for the inclusion of the edge 3^1: [1,4] in the two triangles 1^2: [1,2,4] and 3^2: [1,3,4].

During each run, the downward Hasse diagram is maintained, while a copy of the upward Hasse diagram is updated after the removal of a critical face or of a pair consisting of a free face and the unique face it is contained in. The sequence of updating steps for the above example could be as follows:

0. `compute downward and upward Hasse diagram`
1. `initialize copy of the upward Hasse diagram`
2. `free edges`: none
3. `select random critical triangle:` 5^2: [2,3,4]
4. `update upward Hasse diagram:`

   $i = 1$: $1^1 \nearrow \{1^2, 2^2\}$, $2^1 \nearrow \{3^2, 4^2\}$, $3^1 \nearrow \{1^2, 3^2\}$, $4^1 \nearrow \{2^2, 4^2\}$, $5^1 \nearrow \{6^2\}$, $6^1 \nearrow \{1^2\}$, $7^1 \nearrow \{2^2, 6^2\}$, $8^1 \nearrow \{3^2\}$, $9^1 \nearrow \{4^2, 6^2\}$

5. `free edges:` $5^1, 6^1, 8^1$
6. `select random free edge:` 8^1: [3,4] `paired with` 3^2: [1,3,4]
7. `update upward Hasse diagram:`

   $i = 1$: $1^1 \nearrow \{1^2, 2^2\}$, $2^1 \nearrow \{4^2\}$, $3^1 \nearrow \{1^2, 3^2\}$, $4^1 \nearrow \{2^2, 4^2\}$, $5^1 \nearrow \{6^2\}$, $6^1 \nearrow \{1^2\}$, $7^1 \nearrow \{2^2, 6^2\}$, $8^1 \nearrow \{\}$, $9^1 \nearrow \{4^2, 6^2\}$,

   $i = 0$: $1^0 \nearrow \{1^1, 2^1, 3^1, 4^1\}$, $2^0 \nearrow \{1^1, 5^1, 6^1, 7^1\}$, $3^0 \nearrow \{2^1, 5^1, 9^1\}$, $4^0 \nearrow \{3^1, 6^1\}$, $5^0 \nearrow \{4^1, 7^1, 9^1\}$

8. `free edges:` $2^1, 3^1, 5^1, 6^1$
9. ...

The downward Hasse diagram tells us precisely which parts of the upward Hasse diagram we have to update. For example, the choice of the critical triangle 5^2: [2,3,4] forces us to update, via $5^2 \searrow \{5^1, 6^1, 8^1\}$, the inclusions of the edges $5^1, 6^1, 8^1$ in the upward Hasse diagram (by removing the triangle 5^2 as including face).

Triangulations of closed manifolds initially have no free faces. Thus, we start with an empty list of free faces and immediately remove a random critical face. For triangulations of manifolds with boundary or general simplicial complexes, we first have to initialize the list of free faces. (This extra effort in computation time can be seen by comparing the respective run times for the examples `knot` and `nc_sphere` in Table 3 (see also Section 5.5): With 0.813 seconds, the 3-ball `knot` takes slightly longer per round than the 3-sphere `nc_sphere` with 0.470 seconds.)

Whenever we are done with one level of the Hasse diagram, we initialize the set of free faces for the next level below. Besides updating the upward Hasse diagram in each round, we also keep track of

- the current *list of free faces* (and update this list whenever we delete a critical face or a pair consisting of a free face and the unique face it is contained in),
- the current *discrete Morse vector* $(c_0, c_1, \ldots, c_d)$ (which is initialized by $(0, 0, \ldots, 0)$ and updated by incrementing c_i by one whenever a critical face of dimension i is selected).

At the end of every round, the resulting discrete Morse vector $(c_0, c_1, \ldots, c_d)$ is stored along with its number of appearances in the various rounds. Eventually, we output the list of all obtained discrete Morse vectors together with their frequencies.

2.1 Implementation in GAP

We implemented our random heuristic in GAP [30]. In particular, we used GAP operations on lists and sets to initialize and update Hasse diagrams and respective lists of free faces. Our implementation is basic and has roughly 150 lines of code.

The largest complex (in terms of number of faces) we tested our program on has face vector $f = (5013, 72300, 290944, 495912, 383136, 110880)$ [1]. For this triangulation of a 5-manifold different(!) from a 5-ball it took in total 60:17:33 + 21:41:31 h:min:sec to first build the Hasse

diagram and then to run the random heuristic once, respectively. As resulting discrete Morse vector we obtained $(1, 0, 0, 0, 0, 0)$; thus, this non-trivial 5-manifold is collapsible.

We point out that there is considerable room for improvement with respect to computation time. First of all, the Hasse diagram of a complex can be stored in terms of (sparse) boundary matrices on which fast elimination steps represent elementary collapses; see Joswig [34] for a discussion. In addition, it is way faster to perform matrix operations in, say, C++ compared to elementary set operations in GAP. Nevertheless, if it comes to compute (respectively to simplify a presentation of) the fundamental group of a simplicial complex, then GAP provides efficient heuristics; cf. Section 5.10.

3 Comparison with other algorithms

There are three main previous algorithmic approaches that aim to compute optimal discrete Morse functions for simplicial complexes, one by Joswig and Pfetsch [35], one by Engström [25], and one by Lewiner, Lopes, and Tavares [44] (cf. also Lewiner [43]).

Tools that allow to improve discrete Morse functions were provided by Hersh [33]; and King, Knudson, and Mramor [39] discussed how to improve discrete Morse functions for geometric complexes in $\mathbb{R}^3$.

3.1 The algorithm of Joswig and Pfetsch

This deterministic algorithm, apart from a complete backtrack search, is currently the only available implementation that actually determines optimal discrete Morse functions for all inputs. In the Joswig–Pfetsch approach [35], the problem of finding an optimal discrete Morse function is translated into a maximal matching problem for the underlying graph of the Hasse diagram with an additional acyclicity condition [19, 27]. The acyclic matching problem is then solved as an integer linear program.

For various small instances, the Joswig–Pfetsch approach successfully produces optimal discrete Morse functions [35]. A first case, however, for which the associated integer linear program was too large to handle is for the 16-vertex triangulation `poincare` [14] of the Poincaré homology 3-sphere with $f = (16, 106, 180, 90)$. Joswig and Pfetsch interrupted the computation after one week (although they did not make use of the fact that at least six critical cells are necessary since the fundamental group of the Poincaré homology 3-sphere is non-cyclic; cf. Section 5.9). For the same instance our heuristic found the optimal Morse vector $(1, 2, 2, 1)$ within 0.02 seconds. Also for other small instances our heuristic was much faster, e.g., for Rudin's ball `rudin` [65, 74] with $f = (14, 66, 94, 41)$, Joswig and Pfetsch needed 103.78 seconds to achieve the optimal discrete Morse vector $(1, 0, 0, 0)$, while our heuristic found the optimum in 0.004+0.00107 seconds; cf. Section 5.5.

3.2 The approach by Engström

The elegant approach by Engström [25] is deterministic and fast. Roughly speaking, the idea is to proceed by deleting vertex stars, rather than by deleting pairs of faces. Engström introduces what he calls 'Fourier–Morse theory', a theory based on Kahn–Saks–Sturtevant's notion of non-evasiveness, much like Forman's discrete Morse theory was based on Whitehead's notion of collapsibility. Instead of computing discrete Morse functions, Engström's algorithm computes optimal Fourier–Morse functions, which are *some* discrete Morse functions, but not necessarily the optimal ones among them. In particular, obtaining an output

$(1, 0, \ldots, 0)$ with this algorithm yields a certificate of non-evasiveness, a stronger property than collapsibility; cf. [36].

However, there is a 3-ball with only 12 vertices which has the collapsibility property, but not the non-evasiveness property [12]. As for other examples, Engström obtains $(1, 5, 5, 1)$ as the optimal discrete Fourier–Morse vector for the 16-vertex triangulation of the Poincaré homology 3-sphere `poincare`. Instead, the optimal discrete Morse vector for this example is $(1, 2, 2, 1)$. For Rudin's ball `rudin` Engström found $(1, 2, 2, 0)$ compared to the optimum $(1, 0, 0, 0)$. So using this algorithm, the optimum is often missed, even on triangulations with relatively small size.

3.3 The heuristic of Lewiner, Lopes, and Tavares

The heuristic approach of Lewiner, Lopes, and Tavares [44] (cf. also Lewiner [43]) is fast and was used to produce optimal discrete Morse vectors for several large 2- and 3-dimensional complexes. The problem of finding optimal discrete Morse vectors is reformulated in terms of finding maximal hyperforests of hypergraphs. Then different greedy heuristics are used to obtain large hyperforests.

It has to be remarked, though, that most of the instances listed in [44] and later in [43] are mostly harmless from the point of view of discrete Morse theory; they mainly are 2-dimensional surfaces or shellable 3-dimensional balls and spheres, or products thereof — with the exception of the three more complicated examples `knot`, `nc_sphere`, and `bing` from Hachimori's simplicial complex library [32]. It is precisely on these three examples that the greedy heuristics of Lewiner et al. produce somewhat inconsistent results.

In [44], $(1, 1, 1, 0)$ was obtained for `bing` and `knot`. In [43] on p. 92, `bing` and `knot` appear with $(1, 0, 0, 0)$ without mentioning the improvement with respect to [44]. Moreover, `nc_sphere` is listed on p. 92 of [43] with $(1, 2, 2, 1)$ and it is noted on p. 89: "Trickier, the non-shellable 3-sphere (NC Sphere) is a delicate model since no discrete Morse function can reach the minimal number of critical points for smooth homotopy." This latter statement is false as we found (in 12 out of 10000 runs) the optimal discrete Morse vector $(1, 0, 0, 1)$ for `nc_sphere`; cf. Table 3. In fact, the 3-sphere `nc_sphere` with $f = (381, 2309, 3856, 1928)$ is obtained from the 3-ball `knot` with $f = (380, 1929, 2722, 1172)$ by adding a cone over the boundary of `knot`. By this, every discrete Morse function on `knot` with discrete Morse vector $(1, 0, 0, 0)$ can be used to produce a discrete Morse function with discrete Morse vector $(1, 0, 0, 1)$ on `nc_sphere`. In contrast, it would theoretically be possible to have `knot` with optimal discrete Morse vector $(1, 1, 1, 0)$, while `nc_sphere` has optimal discrete Morse vector $(1, 0, 0, 1)$. The best discrete Morse vector we found in 1000000 runs for `knot` is $(1, 1, 1, 0)$; see Table 3 — whereas, as mentioned above, Lewiner [43] seemed to claim $(1, 0, 0, 0)$ for this example, which would beat our algorithm.

4 Theoretical lower bounds for discrete Morse vectors

In this section, we briefly recall some theoretical lower bounds for minimal discrete Morse vectors. The obstructions for the existence of discrete Morse functions with a certain number of critical cells are of various nature. Here we basically use four different criteria. The first concerns ridge-facet incidences, the second follows from elementary algebraic topology (applied to the Morse complex), the third uses knot theory, and the fourth comes from smooth Morse theory.

4.0.1 Ridge-facet incidences and Euler characteristic

In order for a collapse to start, there need to be free faces. This is how to create a first obstruction, namely by constructing d-dimensional triangulations in which every $(d-1)$-face is contained in two or more d-faces.

The most famous example of this type is the dunce hat, a contractible 2-complex obtained from a single triangle by identifying all three boundary edges in a non-coherent way. In any triangulation of the dunce hat each edge belongs to either two or three triangles; cf. [11]. Hence, the dunce hat cannot be collapsible or, in other words, it cannot have $(1, 0, 0)$ as discrete Morse vector.

The vectors $(1, 0, 1)$ and $(1, 1, 0)$ are also forbidden for the dunce hat. In fact, since each elementary collapse deletes two faces of consecutive dimension, it does not change the Euler characteristic. In particular, the alternating sum of the entries of a discrete Morse vector should always be equal to the Euler characteristic of a complex.

The dunce hat does, however, admit $(1, 1, 1)$ as discrete Morse vector, which is therefore optimal.

4.0.2 The Morse complex

Forman showed that any discrete Morse vector on a simplicial complex C is also the face-vector of a *model* for C, that is, a CW-complex homotopy equivalent to C.

Theorem 3 (Forman [28]) *Assume that some d-complex C admits a discrete Morse function with c_i critical faces of dimension i ($i = 0, \ldots, d$). Then C has a model with c_i i-cells, called* Morse complex*.*

This theorem results in several obstructions. First of all, the i-th (rational) Betti number of an arbitrary CW-complex is always bounded above by its number of i-dimensional cells.

Corollary 4 (Forman's weak Morse inequalities [28]) *Assume that some d-complex C admits a discrete Morse function with c_i critical faces of dimension i ($i = 0, \ldots, d$). Then $c_i \geq \beta_i(C)$ for each i.*

The previous result still holds if we consider homology over a finite field.

Corollary 5 *Assume some d-complex C admits a discrete Morse function with c_i critical faces of dimension i ($i = 0, \ldots, d$). Then $c_i \geq \dim H_i(C; \mathbb{Z}_p)$ for each i and for each prime p.*

Sometimes it is convenient to focus on homotopy groups rather than on homology groups. Recall that the fundamental group of a CW-complex with one 0-cell is completely determined by its 2-skeleton; a presentation of the group can be obtained using the 1-cells as generators and the 2-cells as relators. In particular, if the CW-complex has no 1-cells, its fundamental group must be trivial; and if the CW-complex has only one 1-cell, its fundamental group must be trivial or cyclic.

Corollary 6 *Assume some d-complex C with fundamental group G admits a discrete Morse function with 1 critical face of dimension 0 and c_1 critical faces of dimension 1. Then $c_1 \geq \operatorname{rank}(G)$, the minimal number of generators in a presentation of G. (In particular, if G is non-abelian, then $c_1 \geq 2$.)*

4.0.3 Knot-theoretic obstructions

Obstructions coming from short knots have been considered first by Bing [13], Goodrick [31], and Lickorish [46], and later investigated by the two authors [9, 12, 52] and others. Recall that a knot K inside a triangulation of a 3-sphere is just a 1-dimensional subcomplex homeomorphic to a 1-sphere (or in other words, a closed path in the 1-skeleton.) The *knot group* is the fundamental group of the knot complement inside the sphere. Knot groups are perhaps the main invariant in knot theory.

In the simplest form (that is, for 3-dimensional spheres) the obstructions are of the following type:

Theorem 7 (Lickorish [46]; cf. also [9]) *Assume some triangulated* 3*-sphere* S *admits some discrete Morse function with* c_2 *critical* 2*-faces. Then, for* any *knot* K *inside* S*, one has*

$$c_2 \;\geq\; \operatorname{rank}(G_K) - f_1(K),$$

where G_K *is the knot group of* K *and* $f_1(K)$ *is the number of edges of* K*.*

The previous theorem is usually applied together with the following two well-known facts:
(1) there are knots whose groups have arbitrarily high rank; for example, the knot group of a connected sum of m trefoils has rank $\geq m+1$ (Goodrick [31]);
(2) any knot can be realized with only 3 edges in a suitably triangulated 3-sphere (Bing [13]).

In particular, if we consider a 3-sphere S containing the connected sum of three trefoils realized on three edges, then Theorem 7 yields $c_2 \geq 1$ for all discrete Morse vectors $(1, c_1, c_2, 1)$. Note that $c_1 = c_2$, because of Euler characteristic reasons.

A similar statement can be proven for 3-dimensional balls.

Theorem 8 ([9, Corollary 4.25]) *Assume some triangulated* 3*-ball* B *admits some discrete Morse function with* c_1 *critical edges. Let* K *be a knot in the* 1*-skeleton of* B*, realized as a path of* b *edges in the boundary of* B *plus a path of* $e = f_1(K) - b$ *interior edges. Then*

$$c_1 \;\geq\; \operatorname{rank}(G_K) - 2e,$$

where G_K *is the knot group of* K*.*

4.0.4 Morse-theoretical obstructions

Very recently, the first author proved the following result for smooth manifolds.

Theorem 9 *([10]) Every smooth Morse vector is also a discrete Morse vector on some (compatible) PL triangulation. In dimensions up to* 7*, the converse holds too.*

The converse statement is interesting for us because it yields further obstructions. For example, we know from the work by Boileau and Zieschang [15] and others, that for every $r > 0$, there is a (smooth) 3-manifold M_r of Heegaard genus $g \geq \operatorname{rank}(M_r) + r$. It follows that *for every PL triangulation* T *of* M_r, every discrete Morse vector on T has $c_1 \geq g \geq \operatorname{rank}(M_n) + r$ critical edges.

5 Towards a new library of triangulations

Table 3 provides a library of 45 instances for which we sampled the discrete Morse spectrum. We ran our random algorithm 10000 rounds on each example, except for eight examples for which we did fewer runs. The 45 examples were selected for different reasons as we will explain below. The respective examples are listed at the beginning of each subsection. The library of examples can be found online at [56].

An additional infinite series of complicated triangulations, based on a handlebody construction of Akbulut and Kirby [3], was recently given in [70].

5.1 'Trivial' triangulations

`Examples: dunce_hat, d2n12g6, regular_2_21_23_1`

Discrete Morse theory is trivial on 1-dimensional complexes (graphs) and 2-dimensional compact manifolds (surfaces); cf. [44]. A simple modification of our heuristic allows to incorporate this as follows. Once we reduced a simplicial complex to a 1-dimensional complex, we switch to a deterministic strategy: As long as there are edges that are contained in a cycle, delete such (critical) edges iteratively; then collapse the remaining tree/forest to a point/a collection of points.

Definition 10 *Let C be a connected finite simplicial complex. The* normalized discrete Morse spectrum *of C is obtained from the discrete Morse spectrum of C by normalizing every discrete Morse vector $(c_0, c_1, c_2, \ldots, c_d)$ in the spectrum to $(1, c_1 - c_0 + 1, c_2, \ldots, c_d)$ and adding up the probabilities for the original vectors that have the same normalization.*

Example: The graph A_7 of Figure 1 has normalized discrete Morse spectrum $\{1\text{-}(1,2)\}$ or, for short, $\{(1,2)\}$.

Lemma 11 *Every connected simplicial 1-complex K with n vertices and $m \geq n-1$ edges has normalized discrete Morse spectrum $\{(1, m-n+1)\}$.*

The homology vector in this case is $H_*(K) = (\mathbb{Z}, \mathbb{Z}^{m-n+1})$, so the weak discrete Morse inequalities (see Section 5.9) are sharp.

Lemma 12 *Every triangulation K of a closed (connected) surface of Euler characteristics χ has normalized discrete Morse spectrum $\{(1, 2-\chi, 1)\}$. More generally, the same holds for every strongly connected 2-complex K without free edges.*

Proof: Triangulations of surfaces are strongly connected. Hence, after the removal of only one critical triangle the remaining complex collapses onto a 1-dimensional complex, i.e., $c_2 = 1$. The conclusion follows from the previous lemma and extends to all strongly connected 2-complex K without free edges. □

The example `d2n12g6` in Table 3 is the unique vertex-transitive, vertex-minimal neighborly triangulation of the orientable surface of genus 6 [5], the example `regular_2_21_23_1` is a regular triangulation of the orientable surface of genus 15 with 21 vertices [49, Ch. 5].

Something can also be said on complexes with few vertices:

Theorem 13 (Bagchi and Datta [7]) *Every $\mathbb{Z}_2$-acyclic simplicial complex with at most 7 vertices is collapsible.*

Table 1: Total time to find optimal discrete Morse functions (in a single run) for each of the combinatorial 3-manifolds with up to 10 vertices.

Vertices\Types	S^3	$S^2 \tilde{\times} S^1$	$S^2 \times S^1$	All	Total time (in Min:Sec.Frac)
5	1	–	–	1	0.008
6	2	–	–	2	0.008
7	5	–	–	5	0.012
8	39	–	–	39	0.060
9	1 296	1	–	1 297	3.836
10	247 882	615	518	249 015	17:35.606

Corollary 14 *Every $\mathbb{Z}_2$-acyclic simplicial complex K with at most 7 vertices is extendably collapsible and therefore has trivial discrete Morse spectrum $\{(1,0,0)\}$.*

The 7-vertex bound is sharp; the triangulation `dunce_hat` of the dunce hat is an 8-vertex example of a non-collapsible contractible complex.

5.2 3-manifolds with up to ten vertices

For all 250 359 examples in the catalog [53] of triangulations of 3-manifolds with up to 10 vertices, optimal discrete Morse vectors were found by a *single run* of our program each; see Table 1.

Theorem 15 *All 250 359 examples of triangulated 3-manifolds with up to 10 vertices admit a perfect discrete Morse function.*

The spheres in this list are all shellable, as are all 3-spheres with up to 11 vertices [68]. The smallest known non-shellable 3-sphere `S_3_13_56` (`trefoil`) has 13 vertices [52]. For all the 1134 non-spherical examples the statement of the theorem is new.

5.3 Polytopal spheres

`Examples: S_3_100_4850, 600_cell, S_3_1000_2990, S_5_100_472.`

We ran our program on the 3-dimensional boundary `S_3_100_4850` of the cyclic 4-polytope with 100 vertices and 4850 facets, on the 3-dimensional boundary `600_cell` of the 600-cell, on the 3-dimensional boundary `S_3_1000_2990` of a stacked 4-polytope with 1000 vertices and 2990 facets, and on the 4-dimensional boundary `S_5_100_472` of a stacked 5-polytope with 100 vertices and 472 facets. In all these cases we obtained the optimal discrete Morse vector $(1,0,\ldots,0,1)$ in 10000 out of 10000 tries. We also tested various other examples of simplicial polytopal spheres and we always observed a trivial spectrum in these experiments. However, the normalized discrete Morse spectrum of simplicial polytopal spheres is not trivial in general.

Theorem 16 (Crowley, Ebin, Kahn, Reyfman, White, and Xue [22]) *The 7-simplex Δ_7 with 8 vertices contains in its 2-skeleton an 8-vertex triangulation of the dunce hat onto which it collapses.*

As a direct consequence of Theorem 16, the 7-simplex Δ_7 is *not* extendably collapsible. Therefore the spectrum of its boundary is non-trivial. The same can be said for the simplicial polytopal Grünbaum–Sreedharan 3-sphere No.32, which contains the dunce hat [11].

5.4 Random spheres

`Example: S_3_50_1033.`

While random surfaces can easily be generated, we lack good random models for 3- or higher-dimensional manifolds; cf. [24]. One possible approach is to consider all triangulations of 3-spheres or 3-manifolds with a fixed number n of vertices, with the uniform distribution. While this setting is very promising for performing random experiments, we need to get a hold on the set of all the triangulations with n vertices in the first place, a task that so far has only been solved for 3-manifolds with up to 11 vertices [68].

Another model can be derived by performing random walks on the set of all triangulations where each step is represented by a single bistellar flip. According to a theorem of Pachner [63], two distinct triangulations of a manifold are PL homeomorphic if and only if they can be connected by a sequence of bistellar flips. An implementation of bistellar flips for exploring the space of triangulations within one PL component is the program BISTELLAR [57]; see [14] for a program description. The bistellar flip approach for generating random triangulations depends on the number of executed flips as well as on the way the flips are chosen. As a consequence, triangulations with n vertices are not selected according to the uniform distribution.

For the example `S_3_50_1033`, we started with the boundary of the cyclic 4-polytope with 50 vertices and face vector $f = (50, 1225, 2350, 1175)$. We then applied 1500 bistellar 1-flips and reverse-1-flips that were chosen randomly from all admissible flips. The resulting sphere `S_3_50_1033` has f-vector $(50, 1083, 2066, 1033)$. The average number of critical cells in 10000 runs turned out experimentally to be roughly 3.2 (which is considerably larger than 2). We therefore can conclude heuristically that random spheres tend to have a non-trivial spectrum.

5.5 Knotted triangulations of balls and spheres

`Examples: dunce_hat_in_3_ball, Barnette_sphere, B_3_9_18, trefoil_arc, trefoil, rudin, double_trefoil_arc, double_trefoil, triple_trefoil_arc, triple_trefoil, non_4_2_colorable, knot, nc_sphere, bing.`

The example `dunce_hat_in_3_ball` is a triangulated 3-ball that contains the 8-vertex triangulation `dunce_hat` in its 2-skeleton. To indeed get stuck with `dunce_hat`, we need to perform collapses without removing any of the 17 triangles of the dunce hat. This results in a low probability to get stuck. Indeed, in 1 000 000 runs we always found $(1, 0, 0, 0)$ as resulting discrete Morse vector.

The non-polytopal `Barnette_sphere` [8] with 8 vertices also has trivial observed spectrum: In 1 000 000 runs of our program we obtained the optimal discrete Morse vector $(1, 0, 0, 1)$. For the non-shellable 3-ball `B_3_9_18` [51] with 9 vertices and Rudin's non-shellable 3-ball `rudin` [65, 74] with 14 vertices we achieved the optimal discrete Morse vector $(1, 0, 0, 0)$ in every run. Therefore, non-polytopality and non-shellability not necessarily cause a non-trivial observed spectrum.

If we wish to construct triangulated balls or spheres of small size with a very non-trivial observed spectrum, we need to build in complicated substructures of small size (like complicated knots on few edges) to get stuck at.

Table 2: Average number of critical cells for the knotted spheres and their barycentric subdivisions, based on 10000 random runs.

`trefoil`	2.0778	`double_trefoil`	3.5338	`triple_trefoil`	5.9898
`trefoil_bsd`	2.0202	`double_trefoil_bsd`	3.3414	`triple_trefoil_bsd`	5.7352

The triangulated 3-sphere `trefoil` (`S_3_13_56` [52]) contains a 3-edge trefoil knot in its 1-skeleton and has optimal discrete Morse vector $(1, 0, 0, 1)$. This vector was obtained in roughly 96% of the runs of our heuristic. The triangulated 3-sphere `double_trefoil` (`S_3_16_92` [12]) with optimal discrete Morse vector $(1, 0, 0, 1)$ has a 3-edge double trefoil knot in its 1-skeleton. Here, $(1, 0, 0, 1)$ was achieved only in 40% of the runs. The triangulated 3-sphere `triple_trefoil` (`S_3_18_125` [12]) contains a 3-edge triple trefoil knot in its 1-skeleton and has optimal discrete Morse vector $(1, 1, 1, 1)$, which we found 30% of the time.

The 3-ball `trefoil_arc` is obtained from the 3-sphere `trefoil` by deleting the star of a vertex. It contains the trefoil knot as a spanning arc and has optimal discrete Morse vector $(1, 0, 0, 0)$. The deletion of the star of a vertex from the 3-sphere `double_trefoil` yields the 3-ball `double_trefoil_arc` with the double trefoil knot as spanning arc and optimal discrete Morse vector $(1, 1, 1, 0)$.

For the triple trefoil knot the deletion of a vertex from the 3-sphere `triple_trefoil` yields the 3-ball `triple_trefoil_arc` for which the optimal discrete Morse vector is $(1, 2, 2, 0)$; see Theorem 8. We found this vector in about 60% of the runs.

A larger 3-ball `knot` that has the trefoil knot as spanning arc was constructed (via a pile of cubes) by Hachimori [32]. The best discrete Morse vector we found for `knot` is $(1, 1, 1, 0)$. It might as well be that `knot` admits $(1, 0, 0, 0)$ as optimal discrete Morse vector. The non-constructible 3-sphere `nc_sphere` [32] is obtained from `knot` by adding the cone over the boundary of `knot`. For this example, we found $(1, 0, 0, 1)$ as optimal discrete Morse vector, but only in 12 out of 10000 runs.

The triangulation `bing` is a 3-dimensional thickening of Bing's house with two rooms [13] due to Hachimori [32] (again, via a pile of cubes). It is a 3-ball with 480 vertices for which we found $(1, 0, 0, 0)$ as optimal discrete Morse vector in only 7 out of 10000 runs. We therefore can regard this ball as *barely collapsible*.

A non-$(4, 2)$-colorable triangulation `non_4_2_colorable` of the 3-sphere was constructed in [2] with 167 vertices by using 10 copies of the double trefoil knot. The best discrete Morse vector we found once for this example in 10000 runs is $(1, 2, 2, 1)$. The average number of critical cells for `non_4_2_colorable` computed and normalized over only 10 random runs (for the sake of simplicity) as listed in Table 3 is roughly 25.2.

5.6 Barycentric subdivisions

`Examples: trefoil_bsd, double_trefoil_bsd, triple_trefoil_bsd.`

Interestingly, the barycentric subdivisions `trefoil_bsd`, `double_trefoil_bsd`, and `triple_trefoil_bsd` of the knotted spheres `trefoil`, `double_trefoil`, and `triple_trefoil`, respectively, have a lower observed spectrum than the corresponding original spheres; compare Table 2.

5.7 Standard and exotic PL structures on 4-manifolds

`Examples: CP2, RP4, K3_16, K3_17, RP4_K3_17, RP4_11S2xS2.`

Freedman's classification [29] of simply connected closed topological 4-manifolds settled the 4-dimensional topological Poincaré conjecture. The 4-dimensional smooth Poincaré conjecture, however, is still wide open: Does the 4-dimensional sphere S^4 have a unique differentiable structure or are there exotic 4-spheres that are homeomorphic but not diffeomorphic to S^4? The categories PL and DIFF coincide in dimension 4 (see the survey of Milnor [61] and the references contained therein), and the 4-dimensional smooth Poincaré conjecture therefore can be rephrased on the level of triangulations: Is every triangulation of S^4 PL homeomorphic to the boundary of the 5-simplex?

Exotic structures on simply connected 4-manifolds have been intensively studied over the past years. One main task has been to find smaller and smaller k and l such that the connected sum $(\#k\,\mathbb{C}\mathbf{P}^2)\#(-\#l\,\mathbb{C}\mathbf{P}^2)$ has exotic structures. While it is now known that $\mathbb{C}\mathbf{P}^2\#(-\#2\,\mathbb{C}\mathbf{P}^2)$ [4] admits (infinitely many) exotic structures, the remaining interesting open cases are $\mathbb{C}\mathbf{P}^2\#(-\mathbb{C}\mathbf{P})$, $\mathbb{C}\mathbf{P}^2$, and S^4 (the smooth Poincaré conjecture).

The example `CP2` in Table 3 is the unique vertex-minimal 9-vertex triangulation of $\mathbb{C}\mathbf{P}^2$ due to Kühnel and Banchoff [42] and it carries the standard PL structure.

The constructions of exotic structures are often delicate and it is not straightforward to derive corresponding triangulations. A very explicit example, though not simply connected, is due to Kreck [40].

Theorem 17 (Kreck [40]) *The 4-dimensional manifolds $\mathbb{R}\mathbf{P}^4\#K3$ and $\mathbb{R}\mathbf{P}^4\#(S^2\times S^2)^{\#11}$ are homeomorphic but not diffeomorphic; the constituting components being equipped with the standard smooth structures.*

A 17-vertex triangulation `K3_17` of the K3 surface with the standard PL type is due to Spreer and Kühnel [67]. A vertex-minimal 16-vertex triangulation `K3_16` of the topological K3 surface was previously found by Casella and Kühnel [18]. It is not clear whether the two triangulations are PL homeomorphic — we tried bistellar flips to establish a PL homeomorphism between these two triangulations, but without success.

A vertex-minimal 16-vertex triangulation `RP4` of $\mathbb{R}\mathbf{P}^4$ was obtained in [55] by applying bistellar flips to the 31-vertex standard triangulation of $\mathbb{R}\mathbf{P}^4$ by Kühnel [41].

Let K and L be two triangulated 4-manifolds K and L with n and m vertices, respectively. Their connected sum $K\#L$ (or $K\#-L$ in cases when orientation of the components matters) is obtained from K and L by removing a 4-simplex from each of the triangulations and then gluing together the remainders along the respective boundaries. The resulting triangulation $K\#L$ then has $n+m-5$ vertices. Triangulations of connected sums $(S^2\times S^2)^{\#k}$, $k\geq 2$, are therefore easily constructed from a vertex-minimal 11-vertex triangulation of $S^2\times S^2$ [55] by taking connected sums and then applying bistellar flips to reduce the numbers of vertices. This way, we obtained triangulations of $(S^2\times S^2)^{\#2}$ with 12 vertices (vertex-minimal; c.f. [55]), of $(S^2\times S^2)^{\#3}$ with 14 vertices, of $(S^2\times S^2)^{\#5}$ with 16 vertices, of $(S^2\times S^2)^{\#6}$ with 16 vertices, of $(S^2\times S^2)^{\#9}$ with 18 vertices, and of $(S^2\times S^2)^{\#11}$ with 20 vertices.

Theorem 18 *Let $\mathbb{R}\mathbf{P}^4$, $K3$, and $(S^2\times S^2)^{\#11}$ be equipped with their standard PL structures. The PL 4-manifold $\mathbb{R}\mathbf{P}^4\#K3$ has a triangulation `RP4_K3_17` with $16+17-5=28$ vertices and the PL 4-manifold $\mathbb{R}\mathbf{P}^4\#(S^2\times S^2)^{\#11}$ has a triangulation `RP4_11S2xS2` with $16+20-5=31$ vertices. While the underlying topological manifolds of these PL manifolds are homeomorphic, the respective triangulations are not PL homeomorphic.*

By Theorem 18 we see that homeomorphic but not PL homeomorphic triangulations of 4-manifolds can be constructed with only few vertices. (Most likely, the explicit numbers of vertices in Theorem 18 can be further reduced with bistellar flips. However, this would require a rather extensive search, which is beyond the scope of this article.)

Theorem 19 *The examples* `CP2`*,* `RP4`*,* `K3_16`*,* `K3_17`*,* `RP4_K3_17`*, and* `RP4_11S2xS2` *have perfect discrete Morse functions with* 3*,* 5*,* 24*,* 24*,* 27*, and* 27 *critical cells, respectively.*

Interestingly, the computed discrete Morse spectra of `K3_16` and `K3_17` look rather similar. The same can be said for the pair `RP4_K3_17` and `RP4_11S2xS2`.

5.8 Hom complexes

`Examples: Hom_C5_K4, Hom_n9_655_compl_K4, Hom_C6_compl_K5_small, Hom_C6_compl_K5, Hom_C5_K5.`

Hom complexes of certain graphs provide interesting examples of prodsimplicial manifolds [23]. The prodsimplicial structure allows to easily triangulate these manifolds without adding new vertices.

The 3-dimensional Hom complex `Hom_C5_K4` is a triangulation of the 3-dimensional real projective space $\mathbb{R}\mathbf{P}^3$, the Hom complex `Hom_n9_655_compl_K4` triangulates $(S^2 \times S^1)^{\#13}$.

The 4-dimensional example `Hom_C6_compl_K5_small` with $f = (33, 379, 1786, 2300, 920)$ is obtained from `Hom_C6_compl_K5` with $f = (1920, 30780, 104520, 126000, 50400)$ via bistellar flips. Both examples triangulate $(S^2 \times S^2)^{\#29}$, the first with computed normalized average 63.92, the latter with normalized average 83.0. In only three out of 2000 runs we found the discrete Morse vector $(1, 1, 59, 0, 1)$ for `Hom_C6_compl_K5`, but never the optimum $(1, 0, 58, 0, 1)$. In contrast, both the `lex` and the `rev_lex` heuristics yielded $(1, 0, 58, 0, 1)$. In order to keep the list short, Table 3 only lists 10 random runs for `Hom_C6_compl_K5`.

The Hom complex `Hom_C5_K5` with $f = (1020, 25770, 143900, 307950, 283200, 94400)$ is a triangulation of $S^3 \times S^2$ with normalized average 4.6.

5.9 Higher-dimensional manifolds

`Examples: poincare, hyperbolic_dodecahedral_space, S2xpoincare, SU2_SO3, RP5_24, non_PL, _HP2.`

The 16-vertex triangulation `poincare` [14] of the Poincaré homology 3-sphere with f-vector $f = (16, 106, 180, 90)$ has the binary icosahedral group as its fundamental group. Since this group is non-cyclic, we have $c_2 \geq 2$, and therefore every discrete Morse vector for `poincare` must have at least six critical cells, with $(1, 2, 2, 1)$ being the optimal discrete Morse vector according to Table 3; cf. also Lewiner [45].

For the 21-vertex triangulation `hyperbolic_dodecahedral_space` [60] of the Weber–Seifert hyperbolic dodecahedral space [71] with face vector $f = (21, 193, 344, 172)$ the best discrete Morse vector we found is $(1, 4, 4, 1)$. The fundamental group of this manifold can be presented with 4 generators; see Table 5.

The product triangulation `S2xpoincare` of S^2 (taken as the boundary of a tetrahedron) with `poincare` again has the binary icosahedral group as its fundamental group, inherited from `poincare`; for constructing product triangulations see [54] and references therein. The best discrete Morse vector we found for this examples in 103 out of 1000 runs is $(1, 2, 3, 3, 2, 1)$. (Table 3 list only 20 random runs for `S2xpoincare` to keep the list short.)

The two 5-manifolds $SU2/SO3$ and $\mathbb{R}\mathbf{P}^5$ have homology vectors $(\mathbb{Z}, 0, \mathbb{Z}, \mathbb{Z}, 0, \mathbb{Z})$ and $(\mathbb{Z}, \mathbb{Z}_2, 0, \mathbb{Z}_2, 0, \mathbb{Z})$ and triangulations `SU2_SO3` with 13 vertices and `RP5_24` with 24 vertices, respectively [49, 55]. The 15-vertex triangulation `_HP2` of an 8-dimensional manifold 'like a quaternionic projective plane' by Brehm and Kühnel [16] has homology $(\mathbb{Z}, 0, 0, 0, \mathbb{Z}, 0, 0, 0, \mathbb{Z})$.

Theorem 20 *The triangulations `SU2_SO3`, `RP5_24`, and `_HP2` have optimal discrete Morse vectors* $(1, 0, 1, 1, 0, 1)$, $(1, 1, 1, 1, 1, 1)$, *and* $(1, 0, 0, 0, 1, 0, 0, 0, 1)$, *respectively.*

The 18-vertex non-PL triangulation `non_PL` [14] of the 5-dimensional sphere S^5 admits $(1, 0, 0, 2, 2, 1)$ as discrete Morse vector.

5.10 Random 2-complexes and fundamental groups

`Example: rand2_n25_p0.328`

In generalization of the classical Erdős–Rényi model for random graphs [26], Linial and Meshulam [47] considered random 2-dimensional complexes with complete 1-skeleton on n vertices; every triangle with vertices from the set $\{1, \ldots, n\}$ is then added with probability p independently. Let $Y(n, p)$ be the set of such complexes. For the elements of $Y(n, p)$, Linial and Meshulam proved a sharp threshold for the vanishing of the first homology with $\mathbb{Z}_2$-coefficients,

$$\lim_{n\to\infty} \text{Prob}[\, Y \in Y(n,p) \,|\, H_1(Y, \mathbb{Z}_2) = 0 \,] = \begin{cases} 1 & \text{for} \quad p = \frac{2\log n + \omega(n)}{n}, \\ 0 & \text{for} \quad p = \frac{2\log n - \omega(n)}{n}, \end{cases}$$

for any function $\omega(n) \to \infty$ as $n \to \infty$. Replacing homological connectivity by simple connectivity, Babson, Hoffman, and Kahle [6] showed that there is a range for p for which asymptotically almost surely the complexes $Y \in Y(n, p)$ have non-trivial fundamental groups with trivial abelianizations,

$$\lim_{n\to\infty} \text{Prob}[\, Y \in Y(n,p) \,|\, \pi_1(Y) = 0 \,] = 1 \quad \text{for} \quad p \geq \left(\tfrac{3\log n + \omega(n)}{n}\right)^{\frac{1}{2}},$$

with the exponent $\frac{1}{2}$ being best possible.

More recently, Cohen et al. [21] showed that for $p \ll n^{-1}$ asymptotically almost surely the complexes $Y \in Y(n, p)$ admit a discrete Morse functions with no critical 2-cells.

The example `rand2_n25_p0.328` on $n = 25$ vertices from Table 3 with homology $(\mathbb{Z}, 0, \mathbb{Z}^{475})$ has 751 triangles, each picked with probability $p = 0.328$. We found the optimal discrete Morse vector $(1, 0, 475)$ in 275 out of 10000 runs.

According to Seifert and Threlfall [66, §44], a presentation of the fundamental group of a simplicial complex can be obtained via the edge-path group. For this, a spanning tree of edges is deleted from the 1-skeleton of the complex and each remaining edge contributes a generator to the fundamental group, while each triangle of the 2-skeleton contributes a relator; see [58] for an implementation.

We used the GAP command `SimplifiedFpGroup` to simplify the edge-path group presentation of the fundamental group. The heuristic `SimplifiedFpGroup` not necessarily outputs a minimal presentation of a finitely presented group with the minimal number of generators and relators. Nevertheless, even in the case of huge complexes, `SimplifiedFpGroup` succeeded with recognizing trivial, cyclic (one generator, at most one relator), or free groups (no relators). In Table 5, we list for the examples of Table 3 the number of generators (Ge.) and the

number of relators (Re.) of the initial presentation and the number of generators (SGe.) and the number of relators (SRe.) of the simplified group along with the resulting fundamental group (F. Gr.) and the time it took for the simplification. In Tables 5–7, $F(k)$ denotes the free group with k generators.

In the Tables 6 and 7 we list resulting fundamental groups for random 2-complexes with 25 and 50 vertices, respectively. In these tables, the Linial–Meshulam threshold can be observed quite nicely. For $p = \frac{2\log 25}{25} \approx 0.26$ and $p = \frac{2\log 50}{50} \approx 0.16$, 73 and 75 out of 100 random examples with $n = 25$ and $n = 50$ vertices had trivial fundamental groups, respectively. Thus, for these values of p we precisely are in the range of the slope of the threshold. While most of the examples in the Tables 6 and 7 have free fundamental groups, we found 'non-free' examples (for which their presentations could not be simplified to remove all relators) in the range when p is slightly smaller than $\frac{3}{n}$, the value for which Linial, Meshulam, and Rosenthal [48] constructed acyclic examples as sum complexes.

In our experiments we did not observe the Babson–Hoffmann–Kahle examples with non-trivial fundamental groups that have trivial abelianizations. However, as pointed out by Kenyon, 'exceptional events' can occur for random groups in the case when n is small while the asymptotical behavior can be rather different; cf. [62, pp. 42–43].

5.11 Vertex-homogeneous complexes and the Evasiveness Conjecture

`Example: contractible_vertex_homogeneous.`

As remarked by Kahn, Saks, and Sturtevant [36] we have the following implications for simplicial complexes:

$$\text{non-evasive} \implies \text{collapsible} \implies \text{contractible} \implies \mathbb{Z}\text{-acyclic.}$$

The Evasiveness Conjecture [36] for simplicial complexes states that every vertex-homogeneous non-evasive simplicial complex is a simplex. The first examples of vertex-homogeneous $\mathbb{Z}$-acyclic simplicial complexes different from simplices were given by Oliver (cf. [36]); see [50] for further examples. While join products and other constructions can be used to derive vertex-homogeneous contractible simplicial complexes different from simplices, non-trivial vertex-homogeneous non-evasive examples cannot be obtained this way [72].

The smallest example `contractible_vertex_homogeneous` of a contractible vertex-homogeneous simplicial complex from [50] is 11-dimensional with

$$f = (60, 1290, 12380, 58935, 148092, 220840, 211740, 136155, 59160, 16866, 2880, 225).$$

The best discrete Morse vector we found with the `lex` and the `rev_lex` heuristics for this contractible space is $(1, 0, 0, 4, 8, 4, 0, 0, 0, 0, 0, 0)$. We do not know whether the example is collapsible or not.

Acknowledgments

Thanks to Karim Adiprasito, Herbert Edelsbrunner, Alex Engström, Michael Joswig, Roy Meshulam, Konstantin Mischaikow and Vidit Nanda for helpful discussions and remarks.

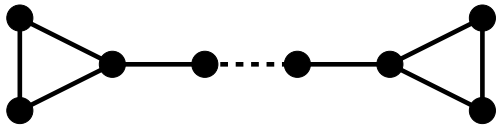

Figure 4: The graph A_{k+6} with $k+6$ vertices.

Appendix A: Complexes on which our heuristic fails

In this section, we construct simplicial complexes on which our random approach will most likely go far from guessing the right Morse vector. On these examples, exponentially many rounds (in the number of facets) of the program may be necessary, before an optimal Morse vector shows up as output. Such pathological examples can be produced in any positive dimension. The crucial idea is highlighted by the following 1-dimensional case.

Example 21 Let k be a positive integer. Let A_{k+6} be the graph consisting of two cycles of length 3 that are connected by a path of k edges; see Figure 4. Since A_{k+6} has no free edge, our algorithm picks an edge e uniformly at random and removes it. The final outcome depends on this choice, and on this choice only:

- If e belongs to the k-edge path, it is easy to see that the program will always output the discrete Morse vector $(2,3)$.
- If instead e belongs to one of the two triangles, then the program will always output the Morse vector $(1,2)$.

Hence, the algorithm finds a perfect Morse function on A_{k+6} with probability $p = \frac{6}{6+k}$. For large k, the algorithm will most likely (i.e. with probability $q = \frac{k}{6+k}$) return a Morse vector that is 'off by 2', displaying 5 critical cells instead of 3.

Example 22 Let s be a positive integer. Let $B_{k+6}(s)$ be a bouquet of s copies of A_{k+6}. An optimal discrete Morse function on $B_{k+6}(s)$ has Morse vector $(1, 2s)$. Finding a discrete Morse function on $B_{k+6}(s)$ is the same as (independently) finding s discrete Morse functions on the s copies of A_{k+6}. Therefore, the probability of getting the optimal Morse vector on $B_{k+6}(s)$ is p^s, where $p = \frac{6}{6+k}$. This corresponds to putting together s optimal Morse functions on the different copies of A_{k+6}, or in other words, to picking one favorable edge in each copy of A_{k+6}. For $0 \leq i \leq s$, the probability that the program outputs the Morse vector $(1+i, 2s+i)$ is $\binom{s}{i} p^{s-i}(1-p)^i$, corresponding to i 'bad choices' and $s-i$ 'good choices'.

To show that an analogous phenomenon occurs also in higher dimensions, let us recall a classical definition in PL topology.

Definition 23 Let C be a d-dimensional complex. A *stacking operation* on C is the transition from C to $C' = (C - \mathrm{star}(\sigma, C)) \cup \hat{\sigma} * \mathrm{link}(\sigma, C)$, where σ is an arbitrary facet of C and $\hat{\sigma}$ is a new vertex (e.g., the barycenter of σ). More generally, we say that C' *is obtained from* C *by stacking* if some finite sequence of stacking operations leads from C to C'.

Each stacking operation adds d facets; so, a complex obtained by performing s stacking operations on a d-simplex has exactly $ds+1$ facets.

Lemma 24 *If C' is obtained from a simplex by stacking, then C' is shellable. In particular, it is endo-collapsible: For any facet σ of C', there is a sequence of elementary collapses that reduces $C' - \sigma$ to $\partial C'$.*

In dimension $d \geq 3$, there is no guarantee that *any* sequence of elementary collapses on $C' - \sigma$ can be continued until one reaches $\partial C'$. This is why, in the following example, probabilities have to be estimated rather than computed.

Example 25 Let d, k be positive integers, with $k \equiv 1 \bmod d$. Take a disjoint union of $d+1$ edges $e_0, \ldots, e_d$, and a d-simplex S (with facets $F_0, \ldots, F_d$). For each i in $\{0, \ldots, d\}$, glue in the boundary of the join $F_i * e_i$. The resulting complex C^d is homotopy equivalent to a bouquet of $d+1$ spheres of dimension d; the homotopy is just the contraction of the central simplex S to a point. Let C^d_k be a complex obtained by stacking the simplex S exactly s times, so that S gets subdivided into $k = ds + 1$ simplices of the same dimension.

Note first of all that C^1_k coincides with the A_{k+6} of Example 21. Since C^d_k has no free $(d-1)$-faces, our algorithm starts by removing some d-face σ at random. We have two possible cases:

- With probability $\frac{k}{(d+2)(d+1)+k}$ we pick σ from the subdivision of the central simplex.
- With probability $\frac{(d+2)(d+1)}{(d+2)(d+1)+k}$ we pick σ from one of the d-spheres.

In the first case, *some* sequence of elementary collapses reduces $C^d_k - \sigma$ onto $d+1$ disjoint d-spheres. So our algorithm will output a Morse vector that is either $(1, 0, \ldots, 1, d+2)$, or a larger vector; but certainly not the vector $(1, 0, \ldots, 0, d+1)$.

Thus the probability of obtaining the optimal Morse vector $(1, 0, \ldots, 0, d+1)$ is positive, but smaller or equal to $\frac{(d+2)(d+1)}{(d+2)(d+1)+k}$. As k gets larger, this upper bound gets smaller and smaller.

Example 26 By taking a bouquet of w copies of Example 25, we obtain a complex $B^d_k(w)$. For $d = 1$, $B^d_k(w)$ coincides with the $B_{k+6}(w)$ of Example 22. The probability of seeing the perfect Morse vector $(1, 0, \ldots, 0, (d+1)w)$ on $B^d_k(w)$ is smaller or equal to $\left(\frac{(d+2)(d+1)}{(d+2)(d+1)+k}\right)^w$.

For practical purposes, it is useful to understand how this probability grows *with respect to the number N of facets*. In fact, given a complex with N facets, we would like to concretely know how often we should run the algorithm before we can expect an optimal Morse vector to appear among the outputs.

For the sake of brevity, we do the calculations in dimension one — but similar estimates can be easily derived in all dimensions. The graph constructed in Example 22 has $N = (6+k)w$ edges. To study the probability $(\frac{6}{6+k})^w$ of finding an optimal Morse function, we should regard N as a constant, write w as $\frac{N}{6+k}$, and study the function

$$P(k) = \left(\frac{6}{6+k}\right)^{\frac{N}{6+k}}.$$

Now, classical calculus reveals that the function $x \longmapsto x^x = e^{x \log x}$ is strictly decreasing on the interval $(0, e^{-1})$ and strictly increasing on (e^{-1}, ∞). It achieves its minimum at e^{-1}. So, given any bijection $g : (0, \infty) \to (0, 1)$, the function $y \longmapsto g(y)^{g(y)}$ achieves its minimum at the (unique) point y such that $g(y) = e^{-1}$. Applying this to $g(y) = \frac{6}{6+y}$, we get

$$\min_{y \in \mathbb{R}} \left(\frac{6}{6+y}\right)^{\frac{N}{6+y}} = \min_{y \in \mathbb{R}} \left(g(y)^{g(y)\frac{N}{6}}\right) = \left(\min_{y \in \mathbb{R}} g(y)^{g(y)}\right)^{\frac{N}{6}} = \left((e^{-1})^{e^{-1}}\right)^{\frac{N}{6}} = e^{-\frac{N}{6e}}.$$

Yet we wanted to minimize the function $P(k)$ over the integers, not over the reals. However, if we choose the integer k so that $\frac{6}{6+k}$ is close to e^{-1}, one can see that the value of $P(k)$ is close to $P(e^{-1})$. The minimum is in fact achieved at $k = 10$. Thus $P(k)$ can be as small as e^{-cN}, where c is some constant 'close' to $\frac{1}{6e}$: It is in fact $c = \frac{1}{16}(\log 8 - \log 3) \approx 0,0613018$.

Appendix B: Library and Tables

Table 3 lists computational results for the examples of Section 5.

Of each example we present the discrete Morse spectrum we experimentally observed in a certain number of runs (usually 10000, when not otherwise stated; sometimes we did fewer runs for reasons concerning either excessive computation time or excessive variance of the spectrum). To sum up in a single coefficient the complicatedness of the spectrum, we introduce the following averages:

- c_σ^N, the average number of critical cells for the vectors in the normalized discrete Morse spectrum of a simplicial complex C;
- $c_{\approx}^N$, the average number of critical cells for a collection of normalized discrete Morse vectors for C.

These two coefficients are of some interest if we want to reduce the size of the complex as a preprocessing step for homology computations. In fact, the second value gives an estimate for the number of cells that we are left with for the Smith normal form computations.

The longer we run Random Discrete Morse, the better the approximation of c_σ^N by $c_{\approx}^N$ will get. If we had an infinite amount of time (and patience), the optimal discrete Morse vectors would eventually show up — as they are always contained in the respective (finite!) discrete Morse spectra.

In Table 3, optimal discrete Morse vectors are highlighted in bold. We wrote an output vector in italics if it is the best we could find with our algorithm and we do not know if it is indeed the optimal or not.

For Table 4, we replaced the random choices in our algorithm with a deterministic lexicographic or reverse lexicographic choice. The labeling of the vertices of course now plays a role; see [59] for a discussion of a randomized version (by randomly renumbering vertices first) of `rev_lex`.

All computations were run on a cluster of 2.6 GHz processors.

Table 3: Library of triangulations and discrete Morse spectra.

Name of example/Homology/ f-vector/$c_{\approx}^N$	Distribution of obtained discrete Morse vectors in 10000 rounds		Time for Hasse diagram/ Time per round (in Hour:Min:Sec.Frac)
`dunce_hat` $(\mathbb{Z}, 0, 0)$ $(8, 24, 17)$ 3.0000	**(1,1,1)**:	10000	0.004 0.00024
`d2n12g6` $(\mathbb{Z}, \mathbb{Z}^{12}, \mathbb{Z})$ $(12, 66, 44)$ 14.0000	**(1,12,1)**: $(2, 13, 1)$: $(3, 14, 1)$:	9722 277 1	0.004 0.00076
`regular_2_21_23_1` $(\mathbb{Z}, \mathbb{Z}^{30}, \mathbb{Z})$ $(21, 147, 98)$ 32.0000	**(1,30,1)**: $(2, 31, 1)$: $(3, 32, 1)$:	9337 649 14	0.008 0.00201
`rand2_n25_p0.328` $(\mathbb{Z}, 0, \mathbb{Z}^{475})$ $(25, 300, 751)$ 482.9032	$(1, 3, 478)$: $(1, 4, 479)$: $(1, 2, 477)$: $(1, 5, 480)$: $(1, 1, 476)$: $(1, 6, 481)$: $(1, 7, 482)$: **(1,0,475)**: $(1, 8, 483)$:	2185 1874 1847 1265 1048 704 318 275 140	0.228 0.00428

Table 3: Library of triangulations and discrete Morse spectra (continued).

Name of example/Homology/ f-vector/$c^N_{\approx}$	Distribution of obtained discrete Morse vectors in 10000 rounds		Time for Hasse diagram/ Time per round (in Hour:Min:Sec.Frac)
	$(2,4,478)$:	66	
	$(2,5,479)$:	66	
	$(2,6,480)$:	54	
	$(2,7,481)$:	41	
	$(1,9,484)$:	40	
	$(2,3,477)$:	24	
	$(2,8,482)$:	21	
	$(1,10,485)$:	12	
	$(2,9,483)$:	8	
	$(1,11,486)$:	4	
	$(2,10,484)$:	3	
	$(2,11,485)$:	3	
	$(3,6,479)$:	1	
	$(3,8,481)$:	1	
`dunce_hat_in_3_ball` $(\mathbb{Z},0,0,0)$ $(8,25,30,12)$ 1.0000	**(1,0,0,0)**:	10000	0.004 0.00049
`Barnette_sphere` (non-polytopal) $(\mathbb{Z},0,0,\mathbb{Z})$ $(8,27,38,19)$ 2.0000	**(1,0,0,1)**:	10000	0.004 0.00060
`B_3_9_18` (non-shellable ball) $(\mathbb{Z},0,0,0)$ $(9,33,43,18)$ 1.0000	**(1,0,0,0)**:	10000	0.004 0.00073
`trefoil_arc` $(\mathbb{Z},0,0,0)$ $(12,58,85,38)$ 1.0952	**(1,0,0,0)**:	9529	0.004 0.00158
	$(1,1,1,0)$:	466	
	$(1,2,2,0)$:	5	
`trefoil` $(\mathbb{Z},0,0,\mathbb{Z})$ $(13,69,112,56)$ 2.0778	**(1,0,0,1)**:	9617	0.004 0.00208
	$(1,1,1,1)$:	377	
	$(1,2,2,1)$:	6	
`rudin` (Rudin's ball) $(\mathbb{Z},0,0,0)$ $(14,66,94,41)$ 1.0000	**(1,0,0,0)**:	10000	0.004 0.00107
`double_trefoil_arc` $(\mathbb{Z},0,0,0)$ $(15,93,145,66)$ 3.6260	**(1,1,1,0)**:	7080	0.012 0.00329
	$(1,2,2,0)$:	2698	
	$(1,3,3,0)$:	197	
	$(2,3,2,0)$:	18	
	$(1,4,4,0)$:	6	
	$(2,4,3,0)$:	1	
`poincare` $(\mathbb{Z},0,0,\mathbb{Z})$ $(16,106,180,90)$ 6.1952	**(1,2,2,1)**:	9073	0.016 0.00400
	$(1,3,3,1)$:	864	
	$(1,4,4,1)$:	45	
	$(2,4,3,1)$:	7	
	$(2,3,2,1)$:	6	
	$(1,5,5,1)$:	5	
`double_trefoil` $(\mathbb{Z},0,0,\mathbb{Z})$ $(16,108,184,92)$ 3.5338	$(1,1,1,1)$:	4550	0.012 0.00408
	(1,0,0,1):	3972	
	$(1,2,2,1)$:	1316	
	$(1,3,3,1)$:	145	
	$(1,4,4,1)$:	8	
	$(2,3,2,1)$:	7	
	$(2,4,3,1)$:	2	

Table 3: Library of triangulations and discrete Morse spectra (continued).

Name of example/Homology/ f-vector/$c^N_{\approx}$	Distribution of obtained discrete Morse vectors in 10000 rounds		Time for Hasse diagram/ Time per round (in Hour:Min:Sec.Frac)
`triple_trefoil_arc` $(\mathbb{Z},0,0,0)$ $(17,127,208,97)$ 5.9352	**(1,2,2,0)**: $(1,3,3,0)$: $(1,4,4,0)$: $(1,5,5,0)$: $(2,4,3,0)$: $(2,3,2,0)$: $(2,5,4,0)$: $(1,6,6,0)$:	6027 3220 569 77 51 42 10 4	0.024 0.00528
`triple_trefoil` $(\mathbb{Z},0,0,\mathbb{Z})$ $(18,143,250,125)$ 5.9898	$(1,2,2,1)$: **(1,1,1,1)**: $(1,3,3,1)$: $(1,4,4,1)$: $(1,5,5,1)$: $(2,3,2,1)$: $(2,4,3,1)$: $(2,5,4,1)$: $(2,6,5,1)$: $(1,6,6,1)$:	4427 3080 1911 430 57 40 33 15 4 3	0.024 0.00640
`hyperbolic_dodecahedral_space` $(\mathbb{Z},\mathbb{Z}_5^3,0,\mathbb{Z})$ $(21,190,338,169)$ 11.4672	*(1,4,4,1)*: $(1,5,5,1)$: $(1,6,6,1)$: $(1,7,7,1)$: $(2,5,4,1)$: $(2,6,5,1)$: $(1,8,8,1)$: $(2,7,6,1)$: $(2,8,7,1)$: $(1,9,9,1)$: $(2,9,8,1)$: $(1,10,10,1)$:	4792 3338 1245 326 82 80 62 45 18 8 3 1	0.036 0.01017
`S_3_50_1033` (random) $(\mathbb{Z},0,0,\mathbb{Z})$ $(50,1083,2066,1033)$ 3.1966	**(1,0,0,1)**: $(1,1,1,1)$: $(1,2,2,1)$: $(1,3,3,1)$: $(1,4,4,1)$: $(1,5,5,1)$: $(1,6,6,1)$: $(2,4,3,1)$: $(2,3,2,1)$: $(2,5,4,1)$: $(1,7,7,1)$: $(2,6,5,1)$: $(1,8,8,1)$: $(2,7,6,1)$: $(2,8,7,1)$: $(1,10,10,1)$: $(2,9,8,1)$: $(1,9,9,1)$:	7087 1383 697 386 189 118 42 25 18 14 12 9 9 4 3 2 1 1	0.900 0.153
`S_3_100_4850` (cyclic polytope) $(\mathbb{Z},0,0,\mathbb{Z})$ $(100,4950,9700,4850)$ 2.0000	**(1,0,0,1)**:	10000	17.829 1.883
`600_cell` $(\mathbb{Z},0,0,\mathbb{Z})$ $(120,720,1200,600)$ 2.0000	**(1,0,0,1)**:	10000	0.364 0.076
`non_4_2_colorable` $(\mathbb{Z},0,0,\mathbb{Z})$ $(167,1579,2824,1412)$ 25.2	$(4,15,12,1)$: $(1,7,7,1)$: $(2,12,11,1)$ $(2,13,12,1)$ $(3,13,11,1)$ $(4,16,13,1)$: $(5,14,10,1)$: $(5,18,14,1)$: $(7,20,14,1)$:	2 1 1 1 1 1 1 1 1	1.728 0.254 [10 rounds]

Table 3: Library of triangulations and discrete Morse spectra (continued).

Name of example/Homology/ f-vector/$c^N_{\approx}$	Distribution of obtained discrete Morse vectors in 10000 rounds		Time for Hasse diagram/ Time per round (in Hour:Min:Sec.Frac)
`Hom_C5_K4` ($\mathbb{R}\mathbf{P}^3$) $(\mathbb{Z}, \mathbb{Z}_2, 0, \mathbb{Z})$ $(240, 1680, 2880, 1440)$ 4.0496	**(1,1,1,1)**: $(1,2,2,1)$: $(2,3,2,1)$: $(1,3,3,1)$:	9753 240 6 1	1.864 0.379
`trefoil_bsd` $(\mathbb{Z}, 0, 0, \mathbb{Z})$ $(250, 1594, 2688, 1344)$ 2.0202	**(1,0,0,1)**: $(1,1,1,1)$: $(1,2,2,1)$:	9902 95 3	1.716 0.308
`knot` $(\mathbb{Z}, 0, 0, 0)$ $(380, 1929, 2722, 1172)$ 3.1194	*(1,1,1,0)*: $(1,2,2,0)$: $(2,3,2,0)$: $(1,3,3,0)$: $(2,4,3,0)$:	9414 560 15 9 2	1.576 0.813
`nc_sphere` $(\mathbb{Z}, 0, 0, \mathbb{Z})$ $(381, 2309, 3856, 1928)$ 4.4760	$(1,1,1,1)$: $(1,2,2,1)$: $(1,3,3,1)$: $(1,4,4,1)$: **(1,0,0,1)**: $(2,3,2,1)$: $(1,6,6,1)$: $(2,4,3,1)$: $(2,5,4,1)$: $(1,5,5,1)$:	7902 1809 234 25 12 9 3 3 2 1	3.228 0.470
`double_trefoil_bsd` $(\mathbb{Z}, 0, 0, \mathbb{Z})$ $(400, 2608, 4416, 2208)$ 3.3414	$(1,1,1,1)$: **(1,0,0,1)**: $(1,2,2,1)$: $(1,3,3,1)$: $(1,4,4,1)$: $(2,3,2,1)$: $(2,4,3,1)$:	4819 4274 833 64 4 4 2	4.376 0.811
`bing` $(\mathbb{Z}, 0, 0, 0)$ $(480, 2511, 3586, 1554)$ 3.0456	$(1,1,1,0)$: $(1,2,2,0)$: **(1,0,0,0)**: $(1,3,3,0)$: $(2,3,2,0)$:	9764 217 7 6 6	2.788 1.398
`triple_trefoil_bsd` $(\mathbb{Z}, 0, 0, \mathbb{Z})$ $(536, 3536, 6000, 3000)$ 5.7352	$(1,2,2,1)$: *(1,1,1,1)*: $(1,3,3,1)$: $(1,4,4,1)$: $(1,5,5,1)$: $(2,3,2,1)$: $(2,4,3,1)$: $(1,6,6,1)$: $(2,5,4,1)$: $(1,8,8,1)$:	4793 3390 1543 208 22 20 17 3 3 1	8.024 1.456
`S_3_1000_2990` (stacked sphere) $(\mathbb{Z}, 0, 0, \mathbb{Z})$ $(1000, 3990, 5980, 2990)$ 2.0000	**(1,0,0,1)**:	10000	8.444 1.498
`Hom_n9_655_compl_K4` ($(S^2 \times S^1)^{\#13}$) $(\mathbb{Z}, \mathbb{Z}^{13}, \mathbb{Z}^{13}, \mathbb{Z})$ $(3096, 22104, 38016, 19008)$ 28.68	**(1,13,13,1)**: $(1,14,14,1)$: $(1,15,15,1)$: $(2,14,13,1)$: $(2,15,14,1)$: $(2,16,15,1)$:	67 20 5 5 2 1	5:39.809 45.682 [100 rounds]
`CP2` $(\mathbb{Z}, 0, \mathbb{Z}, 0, \mathbb{Z})$ $(9, 36, 84, 90, 36)$ 3.0012	**(1,0,1,0,1)**: $(1,1,2,0,1)$:	9994 6	0.012 0.00226

Table 3: Library of triangulations and discrete Morse spectra (continued).

Name of example/Homology/ f-vector/$c^N_{\approx}$	Distribution of obtained discrete Morse vectors in 10000 rounds		Time for Hasse diagram/ Time per round (in Hour:Min:Sec.Frac)
RP4	**(1,1,1,1,1)**:	9765	0.056
$(\mathbb{Z}, \mathbb{Z}_2, 0, \mathbb{Z}_2, 0)$	$(1,2,2,1,1)$:	136	0.01678
$(16, 120, 330, 375, 150)$	$(1,1,2,2,1)$:	89	
5.0490	$(1,3,3,1,1)$:	5	
	$(1,2,3,2,1)$:	3	
	$(1,1,3,3,1)$:	1	
	$(2,3,2,1,1)$:	1	
K3_16 (unknown PL type)	**(1,0,22,0,1)**:	6702	0.168
$(\mathbb{Z}, 0, \mathbb{Z}^{22}, 0, \mathbb{Z})$	$(1,1,23,0,1)$:	2615	0.04417
$(16, 120, 560, 720, 288)$	$(1,2,24,0,1)$:	506	
24.8218	$(1,3,25,0,1)$:	60	
	$(1,0,23,1,1)$:	31	
	$(1,1,24,1,1)$:	15	
	$(1,0,24,2,1)$:	13	
	$(1,0,25,3,1)$:	9	
	$(1,2,25,1,1)$:	6	
	$(2,3,24,0,1)$:	5	
	$(1,0,26,4,1)$:	4	
	$(1,1,26,3,1)$:	4	
	$(1,4,26,0,1)$:	4	
	$(1,0,27,5,1)$:	3	
	$(1,1,27,4,1)$:	3	
	$(1,2,27,3,1)$:	2	
	$(1,3,26,1,1)$:	2	
	$(1,1,28,5,1)$:	2	
	$(1,2,28,4,1)$:	1	
	$(1,3,27,2,1)$:	1	
	$(1,2,29,5,1)$:	1	
	$(1,2,26,2,1)$:	1	
K3_17 (standard PL type)	**(1,0,22,0,1)**:	6337	0.196
$(\mathbb{Z}, 0, \mathbb{Z}^{22}, 0, \mathbb{Z})$	$(1,1,23,0,1)$:	2939	0.05093
$(17, 135, 610, 780, 312)$	$(1,2,24,0,1)$:	618	
24.8978	$(1,3,25,0,1)$:	78	
	$(1,4,26,0,1)$:	8	
	$(1,0,23,1,1)$:	6	
	$(1,0,25,3,1)$:	4	
	$(2,3,24,0,1)$:	3	
	$(1,0,24,2,1)$:	2	
	$(1,0,26,4,1)$:	2	
	$(1,1,24,1,1)$:	1	
	$(1,2,27,3,1)$:	1	
	$(1,5,27,0,1)$:	1	
RP4_K3_17	**(1,1,23,1,1)**:	55	0.392
$(\mathbb{Z}, \mathbb{Z}_2, \mathbb{Z}^{22}, \mathbb{Z}_2, 0)$	$(1,2,24,1,1)$:	24	0.0754
$(28, 245, 930, 1150, 460)$	$(1,3,25,1,1)$:	8	[100 rounds]
28.56	$(1,1,24,2,1)$:	3	
	$(1,2,25,2,1)$:	2	
	$(1,4,26,1,1)$:	2	
	$(1,1,26,4,1)$:	1	
	$(1,3,26,2,1)$:	1	
	$(1,3,27,3,1)$:	1	
	$(1,3,28,4,1)$:	1	
	$(1,5,30,4,1)$:	1	
	$(2,4,25,1,1)$:	1	
RP4_11S2xS2	**(1,1,23,1,1)**:	51	0.496
$(\mathbb{Z}, \mathbb{Z}_2, \mathbb{Z}^{22}, \mathbb{Z}_2, 0)$	$(1,2,24,1,1)$:	29	0.0945
$(31, 283, 1052, 1295, 518)$	$(1,3,25,1,1)$:	14	[100 rounds]
28.46	$(1,1,24,2,1)$:	1	
	$(1,1,25,3,1)$:	1	
	$(1,1,26,4,1)$:	1	
	$(1,2,27,4,1)$:	1	
	$(1,4,26,1,1)$:	1	
	$(2,4,25,1,1)$:	1	

Table 3: Library of triangulations and discrete Morse spectra (continued).

Name of example/Homology/ f-vector/$c^N_{\approx}$	Distribution of obtained discrete Morse vectors in 10000 rounds		Time for Hasse diagram/ Time per round (in Hour:Min:Sec.Frac)
`Hom_C6_compl_K5_small` $((S^2\times S^2)^{\#29})$ $(\mathbb{Z},0,\mathbb{Z}^{58},0,\mathbb{Z})$ $(33,379,1786,2300,920)$ 63.92	$(1,1,59,0,1)$: $(1,2,60,0,1)$: $(1,3,61,0,1)$: **(1,0,58,0,1)**: $(1,4,62,0,1)$: $(1,5,63,0,1)$: $(1,6,64,0,1)$: $(2,3,60,0,1)$: $(1,4,63,1,1)$: $(1,7,65,0,1)$:	33 30 12 11 5 3 3 1 1 1	1.460 0.348 [100 rounds]
`Hom_C6_compl_K5` $((S^2\times S^2)^{\#29})$ $(\mathbb{Z},0,\mathbb{Z}^{58},0,\mathbb{Z})$ $(1920,30780,104520,126000,50400)$ 83.0	$(1,10,68,0,1)$: $(1,17,75,0,1)$: $(1,7,65,0,1)$: $(1,8,66,0,1)$: $(1,9,67,0,1)$: $(1,11,69,0,1)$: $(2,16,73,0,1)$:	3 2 1 1 1 1 1	2:18:33.603 19:26.475 [10 rounds] ([2000 rounds], Sec. 5.8)
`SU2_SO3` $(\mathbb{Z},0,\mathbb{Z},\mathbb{Z},0,\mathbb{Z})$ $(13,78,286,533,468,156)$ 4.1354	**(1,0,1,1,0,1)**: $(1,0,2,2,0,1)$: $(1,1,2,1,0,1)$: $(1,0,3,3,0,1)$: $(1,1,3,2,0,1)$: $(1,0,4,4,0,1)$: $(1,2,3,1,0,1)$:	9369 554 35 32 5 4 1	0.124 0.03250
`non_PL` $(\mathbb{Z},0,0,0,0,\mathbb{Z})$ $(18,139,503,904,783,261)$ 6.1328	*(1,0,0,2,2,1)*: $(1,0,0,3,3,1)$: $(1,0,1,3,2,1)$: $(1,0,0,4,4,1)$: $(1,0,1,4,3,1)$: $(1,0,2,4,2,1)$: $(1,0,0,5,5,1)$: $(1,0,2,5,3,1)$: $(1,1,2,3,2,1)$: $(1,0,4,6,2,1)$:	9383 441 134 23 12 2 2 1 1 1	0.324 0.06964
`RP5_24` $(\mathbb{Z},\mathbb{Z}_2,0,\mathbb{Z}_2,0,\mathbb{Z})$ $(24,273,1174,2277,2028,676)$ 6.1766	**(1,1,1,1,1,1)**: $(1,1,2,2,1,1)$: $(1,2,2,1,1,1)$: $(1,1,1,2,2,1)$: $(1,2,3,2,1,1)$: $(1,1,3,3,1,1)$: $(1,3,3,1,1,1)$: $(1,1,2,3,2,1)$: $(1,2,2,2,2,1)$: $(1,1,1,3,3,1)$: $(1,3,3,2,2,1)$: $(1,3,4,2,1,1)$: $(2,3,2,1,1,1)$: $(2,4,3,1,1,1)$:	9181 344 315 97 21 15 9 6 5 3 1 1 1 1	1.800 0.429
`S2xpoincare` $(\mathbb{Z},0,\mathbb{Z},\mathbb{Z},0,\mathbb{Z})$ $(64,1156,5784,11892,10800,3600)$ 15.70	$(1,3,4,3,2,1)$: $(1,4,6,4,2,1)$: *(1,2,3,3,2,1)*: $(1,2,4,4,2,1)$: $(1,3,5,4,2,1)$: $(1,3,6,5,2,1)$: $(1,2,5,5,2,1)$: $(1,4,7,5,2,1)$: $(1,3,7,6,2,1)$:	6 3 2 2 2 2 1 1 1	46.611 8.460 [20 rounds] ([1000 rounds], Sec. 5.9)
`S_5_100_472` (stacked sphere) $(\mathbb{Z},0,0,0,0,\mathbb{Z})$ $(100,579,1430,1895,1416,472)$ 2.0000	**(1,0,0,0,0,1)**:	10000	1.188 0.309

Table 3: Library of triangulations and discrete Morse spectra (continued).

Name of example/Homology/ f-vector/$c^N_{\approx}$	Distribution of obtained discrete Morse vectors in 10000 rounds	Time for Hasse diagram/ Time per round (in Hour:Min:Sec.Frac)
`Hom_C5_K5` ($S^3 \times S^2$) $(\mathbb{Z}, 0, \mathbb{Z}, \mathbb{Z}, 0, \mathbb{Z})$ $(1020, 25770, 143900, 307950, 283200, 94400)$ 4.6	**(1,0,1,1,0,1)**: 7 $(1, 0, 2, 2, 0, 1)$: 2 $(1, 1, 2, 1, 0, 1)$: 1	16:16:14.156 2:53:37.911 [10 rounds]
`_HP2` $(\mathbb{Z}, 0, 0, 0, \mathbb{Z}, 0, 0, 0, \mathbb{Z})$ $(15, 105, 455, 1365, 3003, 4515, 4230, 2205, 490)$ 3.1212	**(1,0,0,0,1,0,0,0,1)**: 9474 $(1, 0, 0, 1, 2, 0, 0, 0, 1)$: 459 $(1, 0, 0, 2, 3, 0, 0, 0, 1)$: 46 $(1, 0, 0, 3, 4, 0, 0, 0, 1)$: 7 $(1, 0, 0, 0, 2, 1, 0, 0, 1)$: 4 $(1, 0, 1, 2, 2, 0, 0, 0, 1)$: 3 $(1, 0, 1, 4, 4, 0, 0, 0, 1)$: 2 $(1, 0, 1, 1, 1, 0, 0, 0, 1)$: 1 $(1, 0, 0, 1, 5, 3, 0, 0, 1)$: 1 $(1, 0, 2, 2, 1, 0, 0, 0, 1)$: 1 $(1, 0, 0, 1, 6, 4, 0, 0, 1)$: 1 $(1, 0, 0, 4, 5, 0, 0, 0, 1)$: 1	11.348 1.425
`contractible_vertex_homogeneous` $(\mathbb{Z}, 0, 0, 0, 0, 0, 0, 0, 0, 0, 0, 0)$ $(60, 1290, 12380, 58935, 148092, 220840, 211740, 136155, 59160, 16866, 2880, 225)$ 273.6	$(1, 3, 38, 98, 83, 20, 0, \ldots, 0)$: 1 $(1, 3, 42, 72, 43, 10, 0, \ldots, 0)$: 1 $(1, 4, 34, 80, 64, 14, 0, \ldots, 0)$: 1 $(1, 4, 53, 87, 56, 18, 0, \ldots, 0)$: 1 $(1, 5, 63, 110, 61, 9, 0, \ldots, 0)$: 1 $(1, 5, 70, 139, 92, 18, 0, \ldots, 0)$: 1 $(1, 6, 42, 115, 108, 29, 0, \ldots, 0)$: 1 $(1, 8, 75, 160, 113, 20, 0, \ldots, 0)$: 1 $(1, 9, 66, 124, 89, 22, 0, \ldots, 0)$: 1 $(1, 13, 74, 144, 97, 14, 0, \ldots, 0)$: 1	11:42:37.994 1:39:02.745 [10 rounds]

Table 4: Discrete Morse vectors with `lex` and `rev_lex` heuristics.

Name of example	lex	rev_lex
`dunce_hat`	**(1,1,1)**	**(1,1,1)**
`d2n12g6`	**(1,12,1)**	**(1,12,1)**
`regular_2_21_23_1`	**(1,30,1)**	**(1,30,1)**
`rand2_n25_p0.328`	**(1,0,475)**	**(1,0,475)**
`dunce_hat_in_3_ball`	**(1,0,0,0)**	**(1,0,0,0)**
`Barnette_sphere`	**(1,0,0,1)**	**(1,0,0,1)**
`B_3_9_18` (non-shellable ball)	**(1,0,0,0)**	**(1,0,0,0)**
`trefoil_arc`	$(1, 2, 2, 0)$	**(1,0,0,0)**
`trefoil`	$(1, 2, 2, 1)$	**(1,0,0,1)**
`rudin` (Rudin's ball)	**(1,0,0,0)**	**(1,0,0,0)**
`double_trefoil_arc`	$(1, 3, 3, 0)$	$(1, 2, 2, 0)$
`poincare`	**(1,2,2,1)**	**(1,2,2,1)**
`double_trefoil`	$(1, 3, 3, 1)$	$(1, 1, 1, 1)$
`triple_trefoil_arc`	$(1, 4, 4, 0)$	$(1, 3, 3, 0)$
`triple_trefoil`	$(1, 4, 4, 1)$	$(1, 2, 2, 1)$
`hyperbolic_dodecahedral_space`	*(1,4,4,1)*	$(1, 5, 5, 1)$
`S_3_50_1033` (random)	**(1,0,0,1)**	**(1,0,0,1)**
`S_3_100_4850` (cyclic polytope)	**(1,0,0,1)**	**(1,0,0,1)**
`600_cell`	**(1,0,0,1)**	**(1,0,0,1)**
`non_4_2_colorable`	$(1, 30, 30, 1)$	**(1,0,0,1)**
`Hom_C5_K4` ($\mathbb{R}\mathbf{P}^3$)	**(1,1,1,1)**	**(1,1,1,1)**
`trefoil_bsd`	$(1, 2, 2, 1)$	**(1,0,0,1)**
`knot`	*(1,1,1,0)*	*(1,1,1,0)*
`nc_sphere`	$(1, 2, 2, 1)$	$(1, 1, 1, 1)$
`double_trefoil_bsd`	$(1, 3, 3, 1)$	$(1, 1, 1, 1)$
`bing`	$(1, 1, 1, 0)$	$(1, 1, 1, 0)$
`triple_trefoil_bsd`	$(1, 4, 4, 1)$	$(1, 3, 3, 1)$
`S_3_1000_2990` (stacked sphere)	**(1,0,0,1)**	**(1,0,0,1)**
`Hom_n9_655_compl_K4` ($(S^2 \times S^1)^{\#13}$)	(2,14,13,1)	**(1,13,13,1)**

Table 4: Discrete Morse vectors with `lex` and `rev_lex` heuristics (continued).

Name of example	lex	rev_lex
CP2	**(1,0,1,0,1)**	**(1,0,1,0,1)**
RP4	**(1,1,1,1,1)**	**(1,1,1,1,1)**
K3_16 (unknown PL type)	**(1,0,22,0,1)**	**(1,0,22,0,1)**
K3_17 (standard PL type)	**(1,0,22,0,1)**	**(1,0,22,0,1)**
RP4_K3_17	**(1,1,23,1,1)**	**(1,1,23,1,1)**
RP4_11S2xS2	**(1,1,23,1,1)**	**(1,1,23,1,1)**
Hom_C6_compl_K5_small ($(S^2\times S^2)^{\#29}$)	**(1,0,58,0,1)**	**(1,0,58,0,1)**
Hom_C6_compl_K5 ($(S^2\times S^2)^{\#29}$)	**(1,0,58,0,1)**	**(1,0,58,0,1)**
SU2_SO3	**(1,0,1,1,0,1)**	**(1,0,1,1,0,1)**
non_PL	*(1,0,0,2,2,1)*	*(1,0,0,2,2,1)*
RP5_24	**(1,1,1,1,1,1)**	**(1,1,1,1,1,1)**
S2xpoincare	*(1,2,3,3,2,1)*	*(1,2,3,3,2,1)*
S_5_100_472 (stacked sphere)	**(1,0,0,0,0,1)**	**(1,0,0,0,0,1)**
Hom_C5_K5 ($S^3\times S^2$)	**(1,0,1,1,0,1)**	**(1,0,1,1,0,1)**
_HP2	**(1,0,0,0,1,0,0,0,1)**	**(1,0,0,0,1,0,0,0,1)**
contractible_vertex_homogeneous	*(1,0,0,4,8,4,0,0,0,0,0,0)*	*(1,0,0,4,8,4,0,0,0,0,0,0)*

Table 5: Simplified presentations of fundamental groups with GAP.

Name of example	Ge.	Re.	SGe.	SRe.	F. Gr.	Time
dunce_hat	17	17	0	0	0	0.036
d2n12g6	55	44	12	1	12 gen.	0.132
regular_2_21_23_1	127	98	30	1	30 gen.	0.304
rand2_n25_p0.328	276	751	0	0	0	0.876
dunce_hat_in_3_ball	18	30	0	0	0	0.044
Barnette_sphere	20	38	0	0	0	0.048
B_3_9_18 (non-shellable ball)	25	43	0	0	0	0.048
trefoil_arc	47	85	0	0	0	0.092
trefoil	57	112	0	0	0	0.084
rudin (Rudin's ball)	53	94	0	0	0	0.060
double_trefoil_arc	79	145	0	0	0	0.148
poincare	91	180	2	2	2 gen.	0.104
double_trefoil	93	184	0	0	0	0.160
triple_trefoil_arc	111	208	0	0	0	0.164
triple_trefoil	126	250	0	0	0	0.156
hyperbolic_dodecahedral_space	170	338	4	5	4 gen.	0.276
S_3_50_1033 (random)	1034	2066	0	0	0	6.372
S_3_100_4850 (cyclic polytope)	4851	9700	0	0	0	2:38.918
600_cell	601	1200	0	0	0	2.220
non_4_2_colorable	1413	2824	0	0	0	12.644
Hom_C5_K4 ($\mathbb{R}\mathbf{P}^3$)	1441	2880	1	1	$\mathbb{Z}_2$	13.492
trefoil_bsd	1345	2688	0	0	0	11.292
knot	1550	2722	0	0	0	12.536
nc_sphere	1929	3856	0	0	0	23.509
double_trefoil_bsd	2209	4416	0	0	0	30.002
bing	2032	3586	0	0	0	22.877
triple_trefoil_bsd	3001	6000	0	0	0	57.947
S_3_1000_2990 (stacked sphere)	2991	5980	0	0	0	58.099
Hom_n9_655_compl_K4 ($(S^2\times S^1)^{\#13}$)	19009	38016	13	0	F(13)	59:14.006
CP2	28	84	0	0	0	0.036
RP4	105	330	1	1	$\mathbb{Z}_2$	0.200
K3_16 (unknown PL type)	105	560	0	0	0	0.344
K3_17 (standard PL type)	119	610	0	0	0	0.372
RP4_K3_17	218	930	0	0	$\mathbb{Z}_2$	0.408
RP4_11S2xS2	253	1052	0	0	$\mathbb{Z}_2$	0.472
Hom_C6_compl_K5_small ($(S^2\times S^2)^{\#29}$)	347	1786	0	0	0	2.420
Hom_C6_compl_K5 ($(S^2\times S^2)^{\#29}$)	28861	104520	0	0	0	3:57:09.873
SU2_SO3	66	286	0	0	0	0.180
non_PL	122	503	0	0	0	0.368
RP5_24	250	1174	1	1	$\mathbb{Z}_2$	1.244
S2xpoincare	1093	5784	2	2	2 gen.	22.493
S_5_100_472 (stacked sphere)	480	1430	0	0	0	2.380
Hom_C5_K5 ($S^3\times S^2$)	24751	143900	0	0	0	5:22:22.520
_HP2	91	455	0	0	0	0.356
contractible_vertex_homogeneous	1231	12380	0	0	0	46.431

Table 6: Distribution of fundamental groups for random 2-complexes with 25 vertices (100 runs for each p).

p	0	$F(1)$	$F(2)$	$F(3)$	$F(4)$	$F(5)$	$F(6)$	$F(7)$	$F(8)$	$F(9)$	$F(10)$	$F(\geq 11)$	'non-free'
0.40	100	0	0	0	0	0	0	0	0	0	0	0	0
0.39	100	0	0	0	0	0	0	0	0	0	0	0	0
0.38	99	1	0	0	0	0	0	0	0	0	0	0	0
0.37	100	0	0	0	0	0	0	0	0	0	0	0	0
0.36	98	2	0	0	0	0	0	0	0	0	0	0	0
0.35	96	3	1	0	0	0	0	0	0	0	0	0	0
0.34	99	1	0	0	0	0	0	0	0	0	0	0	0
0.33	97	3	0	0	0	0	0	0	0	0	0	0	0
0.32	95	5	0	0	0	0	0	0	0	0	0	0	0
0.31	97	3	0	0	0	0	0	0	0	0	0	0	0
0.30	97	3	0	0	0	0	0	0	0	0	0	0	0
0.29	88	10	1	1	0	0	0	0	0	0	0	0	0
0.28	83	16	1	0	0	0	0	0	0	0	0	0	0
0.27	83	15	2	0	0	0	0	0	0	0	0	0	0
0.26	73	19	8	0	0	0	0	0	0	0	0	0	0
0.25	73	21	3	2	1	0	0	0	0	0	0	0	0
0.24	66	27	6	1	0	0	0	0	0	0	0	0	0
0.23	39	39	20	1	1	0	0	0	0	0	0	0	0
0.22	31	39	20	8	2	0	0	0	0	0	0	0	0
0.21	23	24	35	7	7	2	1	0	1	0	0	0	0
0.20	16	33	26	16	5	3	1	0	0	0	0	0	0
0.19	8	18	24	16	18	7	7	1	0	1	0	0	0
0.18	9	13	24	18	19	8	3	1	4	1	0	0	0
0.17	2	6	10	20	9	21	13	10	5	3	0	1	0
0.16	0	1	3	13	12	17	21	9	6	4	6	8	0
0.15	0	0	0	4	16	5	10	14	10	10	7	24	0
0.14	0	0	0	0	0	1	3	5	11	13	5	62	0
0.13	0	0	0	0	0	0	1	1	0	3	6	89	0
0.12	0	0	0	0	0	0	0	0	0	0	3	96	1
0.11	0	0	0	0	0	0	0	0	0	0	0	92	8
0.10	0	0	0	0	0	0	0	0	0	0	0	98	2
0.09	0	0	0	0	0	0	0	0	0	0	0	99	1
0.08	0	0	0	0	0	0	0	0	0	0	0	100	0
0.07	0	0	0	0	0	0	0	0	0	0	0	100	0
0.06	0	0	0	0	0	0	0	0	0	0	0	100	0

References

[1] K. Adiprasito, B. Benedetti, and F. H. Lutz. Random discrete Morse theory and manifold recognition. In preparation.

[2] K. Adiprasito, J. Cibulka, J. Kynčl, F. H. Lutz, J. Møller, and M. Tancer. Work in progress.

[3] S. Akbulut and R. Kirby. A potential smooth counterexample in dimension 4 to the Poincaré conjecture, the Schoenflies conjecture, and the Andrews–Curtis conjecture. *Topology* **24**, 375–390 (1985).

[4] A. Akhmedov and B. D. Park. Exotic smooth structures on small 4-manifolds with odd signatures. *Invent. Math.* **181**, 577–603 (2010).

[5] A. Altshuler, J. Bokowski, and P. Schuchert. Neighborly 2-manifolds with 12 vertices. *J. Comb. Theory, Ser. A* **75**, 148–162 (1996).

[6] E. Babson, C. Hoffman, and M. Kahle. The fundamental group of random 2-complexes. *J. Am. Math. Soc.* **24**, 1–28 (2010).

Table 7: Distribution of fundamental groups for random 2-complexes with 50 vertices (100 runs for each p).

p	0	$F(1)$	$F(2)$	$F(3)$	$F(4)$	$F(5)$	$F(6)$	$F(7)$	$F(8)$	$F(9)$	$F(10)$	$F(\geq 11)$	'non-free'
0.25	100	0	0	0	0	0	0	0	0	0	0	0	0
0.24	100	0	0	0	0	0	0	0	0	0	0	0	0
0.23	99	1	0	0	0	0	0	0	0	0	0	0	0
0.22	99	1	0	0	0	0	0	0	0	0	0	0	0
0.21	97	3	0	0	0	0	0	0	0	0	0	0	0
0.20	98	2	0	0	0	0	0	0	0	0	0	0	0
0.19	96	4	0	0	0	0	0	0	0	0	0	0	0
0.18	90	10	0	0	0	0	0	0	0	0	0	0	0
0.17	81	18	1	0	0	0	0	0	0	0	0	0	0
0.16	75	24	1	0	0	0	0	0	0	0	0	0	0
0.15	68	26	4	2	0	0	0	0	0	0	0	0	0
0.14	43	27	21	8	1	0	0	0	0	0	0	0	0
0.13	16	39	31	10	2	1	1	0	0	0	0	0	0
0.12	8	15	22	19	25	6	3	1	1	0	0	0	0
0.11	1	4	9	10	16	20	21	8	7	1	1	2	0
0.10	0	0	1	4	5	6	13	17	11	15	10	18	0
0.09	0	0	0	0	1	0	2	0	4	4	5	84	0
0.08	0	0	0	0	0	0	0	0	0	0	0	100	0
0.07	0	0	0	0	0	0	0	0	0	0	0	100	0
0.06	0	0	0	0	0	0	0	0	0	0	0	95	5
0.05	0	0	0	0	0	0	0	0	0	0	0	86	14
0.04	0	0	0	0	0	0	0	0	0	0	0	100	0
0.03	0	0	0	0	0	0	0	0	0	0	0	100	0
0.02	0	0	0	0	0	0	0	0	0	0	0	100	0
0.01	0	0	0	0	0	0	0	0	0	0	0	100	0

[7] B. Bagchi and B. Datta. Combinatorial triangulations of homology spheres. *Discrete Math.* **305**, 1–17 (2005).

[8] D. Barnette. The triangulations of the 3-sphere with up to 8 vertices. *J. Comb. Theory, Ser. A* **14**, 37–52 (1973).

[9] B. Benedetti. Discrete Morse theory for manifolds with boundary. *Trans. Am. Math. Soc.* **364**, 6631–6670 (2012).

[10] B. Benedetti. Smoothing discrete Morse theory. `arXiv:1212.0885v2`, 2013, 27 pages.

[11] B. Benedetti and F. H. Lutz. The dunce hat and a minimal non-extendably collapsible 3-ball. `arXiv:0912.3723v2`, 2013, 6 pages; *Electronic Geometry Models*, to appear.

[12] B. Benedetti and F. H. Lutz. Knots in collapsible and non-collapsible balls. `arXiv:1303.2070`, 2013, 25 pages.

[13] R. H. Bing. Some aspects of the topology of 3-manifolds related to the Poincaré conjecture. *Lectures on Modern Mathematics, Volume II* (T. L. Saaty, ed.), Chapter 3, 93–128. John Wiley & Sons, New York, NY, 1964.

[14] A. Björner and F. H. Lutz. Simplicial manifolds, bistellar flips and a 16-vertex triangulation of the Poincaré homology 3-sphere. *Exp. Math.* **9**, 275–289 (2000).

[15] M. Boileau and H. Zieschang. Heegaard genus of closed orientable Seifert 3-manifolds. *Invent. Math.* **76**, 455–468 (1984).

[16] U. Brehm and W. Kühnel. 15-vertex triangulations of an 8-manifold. *Math. Ann.* **294**, 167–193 (1992).

[17] CAPD::RedHom. Redhom software library. `http://redhom.ii.uj.edu.pl`.

[18] M. Casella and W. Kühnel. A triangulated K3 surface with the minimum number of vertices. *Topology* **40**, 753–772 (2001).

[19] M. K. Chari. On discrete Morse functions and combinatorial decompositions. *Discrete Math.* **217**, 101–113 (2000).

[20] CHomP. *C*omputational *Hom*ology *P*roject. `http://chomp.rutgers.edu`.

[21] D. Cohen, A. Costa, M. Farber, and T. Kappeler. Topology of random 2-complexes. *Discrete Comput. Geom.* **47**, 117–149 (2012).

[22] K. Crowley, A. Ebin, H. Kahn, P. Reyfman, J. White, and M. Xue. Collapsing a simplex to a noncollapsible simplicial complex. Preprint, 2003, 7 pages.

[23] P. Csorba and F. H. Lutz. Graph coloring manifolds. *Algebraic and Geometric Combinatorics,* Euroconf. Math., Algebraic and Geometric Combinatorics, Anogia, Crete, Greece, 2005 (C. A. Athanasiadis, V. V. Batyrev, D. I. Dais, M. Henk, and F. Santos, eds.). Contemporary Mathematics **423**, 51–69. American Mathematical Society, Providence, RI, 2006.

[24] N. M. Dunfield and W. P. Thurston. Finite covers of random 3-manifolds. *Invent. Math.* **166**, 457–521 (2006).

[25] A. Engström. Discrete Morse functions from Fourier transforms. *Exp. Math.* **18**, 45–53 (2009).

[26] P. Erdős and A. Rényi. On the evolution of random graphs. *Publ. Math. Inst. Hung. Acad. Sci., Ser. A* **5**, 17–61 (1960).

[27] R. Forman. Morse theory for cell complexes. *Adv. Math.* **134**, 90–145 (1998).

[28] R. Forman. A user's guide to discrete Morse theory. *Sémin. Lothar. Comb.* **48**, B48c, 35 p., electronic only (2002).

[29] M. H. Freedman. The topology of four-dimensional manifolds. *J. Differ. Geom.* **17**, 357–453 (1982).

[30] The GAP Group. GAP — Groups, Algorithms, and Programming, Version 4.4.12. `http://www.gap-system.org`, 2008.

[31] R. E. Goodrick. Non-simplicially collapsible triangulations of I^n. *Proc. Camb. Phil. Soc.* **64**, 31–36 (1968).

[32] M. Hachimori. Simplicial complex library. `http://infoshako.sk.tsukuba.ac.jp/~hachi/math/library`

[33] P. Hersh. On optimizing discrete Morse functions. *Adv. Appl. Math.* **35**, 294–322 (2005).

[34] M. Joswig. Computing invariants of simplicial manifolds. `arXiv:math.AT/0401176`, 2004, 13 pages.

[35] M. Joswig and M. E. Pfetsch. Computing optimal Morse matchings. *SIAM J. Discrete Math.* **20**, 11–25 (2006).

[36] J. Kahn, M. Saks, and D. Sturtevant. A topological approach to evasiveness. *Combinatorica* **4**, 297–306 (1984).

[37] V. Kaibel and M. E. Pfetsch. Computing the face lattice of a polytope from its vertex-facet incidences. *Comput. Geom.* **23**, 281–290 (2002).

[38] V. Kaibel and M. E. Pfetsch. Some algorithmic problems in polytope theory. *Algebra, Geometry, and Software Systems* (M. Joswig and N. Takayama, eds.), 23–47. Springer-Verlag, Berlin, 2003.

[39] H. King, K. Knudson, and N. Mramor. Generating discrete Morse functions from point data. *Exp. Math.* **14**, 435–444 (2005).

[40] M. Kreck. Some closed 4-manifolds with exotic differentiable structure. *Algebraic Topology, Aarhus 1982,* Proc. conference held in Aarhus, Denmark, 1982 (I. Madsen and B. Oliver, eds.). Lecture Notes in Mathematics **1051**, 246–262. Springer-Verlag, Berlin, 1984.

[41] W. Kühnel. Minimal triangulations of Kummer varieties. *Abh. Math. Sem. Univ. Hamburg* **57**, 7–20 (1987).

[42] W. Kühnel and T. F. Banchoff. The 9-vertex complex projective plane. *Math. Intell.* **5**, No. 3, 11–22 (1983).

[43] T. Lewiner. *Geometric Discrete Morse Complexes.* Dissertation. Pontifícia Universidade Católica do Rio de Janeiro, 2005, 131 pages. `http://zeus.mat.puc-rio.br/tomlew/pdfs/tomlew_phd_puc.pdf`.

[44] T. Lewiner, H. Lopes, and G. Tavares. Optimal discrete Morse functions for 2-manifolds. *Comput. Geom.* **26**, 221–233 (2003).

[45] T. Lewiner, H. Lopes, and G. Tavares. Toward optimality in discrete Morse theory. *Exp. Math.* **12**, 271–285 (2003).

[46] W. B. R. Lickorish. Unshellable triangulations of spheres. *Eur. J. Comb.* **12**, 527–530 (1991).

[47] N. Linial and R. Meshulam. Homological connectivity of random 2-complexes. *Combinatorica* **26**, 475–487 (2006).

[48] N. Linial, R. Meshulam, and M. Rosenthal. Sum complexes—a new family of hypertrees. *Discrete Comput. Geom.* **44**, 622–636 (2010).

[49] F. H. Lutz. *Triangulated Manifolds with Few Vertices and Vertex-Transitive Group Actions.* Dissertation. Shaker Verlag, Aachen, 1999, 146 pages.

[50] F. H. Lutz. Examples of $\mathbb{Z}$-acyclic and contractible vertex-homogeneous simplicial complexes. *Discrete Comput. Geom.* **27**, 137–154 (2002).

[51] F. H. Lutz. A vertex-minimal non-shellable simplicial 3-ball with 9 vertices and 18 facets. *Electronic Geometry Model* No. 2003.05.004 (2004). `http://www.eg-models.de/2003.05.004`.

[52] F. H. Lutz. Small examples of nonconstructible simplicial balls and spheres. *SIAM J. Discrete Math.* **18**, 103–109 (2004).

[53] F. H. Lutz. Combinatorial 3-manifolds with 10 vertices. *Beitr. Algebra Geom.* **49**, 97–106 (2008).

[54] F. H. Lutz. Triangulated Manifolds with Few Vertices: Geometric 3-Manifolds. `arXiv:math.GT/0311116`, 2003, 48 pages.

[55] F. H. Lutz. Triangulated Manifolds with Few Vertices: Combinatorial Manifolds. `arXiv:math.CO/0506372`, 2005, 37 pages.

[56] F. H. Lutz. The Manifold Page, 1999–2013. `http://page.math.tu-berlin.de/~lutz/stellar/`.

[57] F. H. Lutz. `BISTELLAR`, Version Nov/2003. `http://page.math.tu-berlin.de/~lutz/stellar/BISTELLAR` 2003.

[58] F. H. Lutz. `FundamentalGroup`, Version Nov/2003. `http://page.math.tu-berlin.de/~lutz/stellar/FundamentalGroup`, 2003.

[59] F. H. Lutz, K. Mischaikow, and V. Nanda. Work in progress.

[60] F. H. Lutz, T. Sulanke, and E. Swartz. f-vectors of 3-manifolds. *Electron. J. Comb.* **16**, No. 2, Research Paper R13, 33 p. (2009).

[61] J. Milnor. Differential topology forty-six years later. *Notices Am. Math. Soc.* **58**, 804–809 (2011).

[62] Y. Ollivier. *A January 2005 Invitation to Random Groups*. Ensaios Matemáticos **10**. Sociedade Brasileira de Matemática, Rio de Janeiro, 2005.

[63] U. Pachner. Konstruktionsmethoden und das kombinatorische Homöomorphieproblem für Triangulationen kompakter semilinearer Mannigfaltigkeiten. *Abh. Math. Sem. Univ. Hamburg* **57**, 69–86 (1987).

[64] Perseus. The persistent homology software. `http://www.math.rutgers.edu/~vidit/perseus.html`.

[65] M. E. Rudin. An unshellable triangulation of a tetrahedron. *Bull. Am. Math. Soc.* **64**, 90–91 (1958).

[66] H. Seifert and W. Threlfall. *Lehrbuch der Topologie*. B. G. Teubner, Leipzig, 1934.

[67] J. Spreer and W. Kühnel. Combinatorial properties of the $K3$ surface: Simplicial blowups and slicings. *Exp. Math.* **20**, 201–216 (2011).

[68] T. Sulanke and F. H. Lutz. Isomorphism free lexicographic enumeration of triangulated surfaces and 3-manifolds. *Eur. J. Comb.* **30**, 1965–1979 (2009).

[69] M. Tancer. Recognition of collapsible complexes is NP-complete. `arXiv:1211.6254`, 2012, 21 pages.

[70] M. Tsuruga and F. H. Lutz. Constructing complicated spheres. arXiv:1302.6856, 2013, 4 pages, EuroCG 2013.

[71] C. Weber and H. Seifert. Die beiden Dodekaederräume. *Math. Z.* **37**, 237–253 (1933).

[72] V. Welker. Constructions preserving evasiveness and collapsibility. *Discrete Math.* **207**, 243–255 (1999).

[73] J. H. C. Whitehead. Simplicial spaces, nuclei and m-groups. *Proc. Lond. Math. Soc., II. Ser.* **45**, 243–327 (1939).

[74] R. F. Wotzlaw. Rudin's non-shellable ball. *Electronic Geometry Model* No. 2004.08.001 (2005). http://www.eg-models.de/2004.08.001.

Bruno Benedetti
Institut für Informatik
Freie Universität Berlin
Takustr. 9
14195 Berlin, Germany
bruno@zedat.fu-berlin.de

Frank H. Lutz
Institut für Mathematik
Technische Universität Berlin
Straße des 17. Juni 136
10623 Berlin, Germany
lutz@math.tu-berlin.de